Myocardial Contrast Echocardiography
A 25-Year Retrospective

Sanjiv Kaul, MD

Obstacles are those frightful things you see when you take your eyes off your goals.

–Anonymous

In 1997, I wrote an invited review on myocardial contrast echocardiography (MCE) entitled "Myocardial Contrast Echocardiography: 15 Years of Research and Development" in the From-Bench-to-Bedside section of *Circulation*.[1] Then, in 2003, Hiroshi Ito and I wrote a 2-piece invited review entitled "Microvasculature in Acute Myocardial Ischemia: Evolving Concepts in Pathophysiology, Diagnosis, and Treatment" in the Clinical Cardiology: New Frontiers section of *Circulation*.[2,3] In this review for the New Drugs and Technology section of *Circulation*, I will provide a 25-year retrospective on MCE but with emphasis on more recent developments and remaining challenges for the field. I will limit myself to myocardial imaging and will not discuss imaging of other organs or the vascular system. Likewise, I will not address the therapeutic applications of microbubble-ultrasound interactions such as drug and gene delivery or sonothrombolysis.

I have organized this review into 7 sections. I begin by briefly describing some historical and technical elements so that the reader unfamiliar with MCE will be able to follow the rest of the review. I then describe the more recent studies relating to the role of MCE in the diagnosis and prognostication in acute coronary syndromes and chronic coronary artery disease (CAD), followed by assessment of myocardial viability in chronic CAD. After that, I describe advances in site-targeted or molecular imaging and certain miscellaneous findings. Finally, I discuss the remaining challenges of MCE from a clinical adoption point of view.

Some Historical and Technical Elements

Initial MCE studies were performed in dogs to define in vivo the area at risk during acute coronary occlusion with the use of hand-agitated solutions.[4–9] Shortly thereafter, the technique of sonication was described, which allowed the production of smaller microbubbles,[10] and was rapidly adopted for intracoronary injections in animals and humans.[11–13] Subsequently, the first commercial agent (Albunex) was developed by sonication of 5% human albumin solution, and it produced excellent myocardial opacification on intracoronary injection.[14] It therefore came as a surprise to many when this agent was not that successful in opacifying the left ventricular (LV) cavity after intravenous injection.[15]

The gas contained in Albunex microbubbles was air that, being highly diffusible, leaked out of the microbubbles as they crossed the pulmonary circulation, thus reducing their size. Also being highly soluble, the air dissolved in blood very rapidly after leaking out. Because the acoustic backscatter from a bubble is related to the sixth power of its radius, even modest changes in bubble size can result in large changes in backscatter, which explained the poor LV cavity opacification after intravenous administration of Albunex. To overcome this limitation, the air in the bubble was changed to higher-molecular-weight gases (such as fluorocarbons) that resulted in more stable bubbles. Being insoluble in blood, the gas, even when it had escaped from the bubble, continued to produce effective ultrasound backscatter by acting as a free gas bubble.[16,17] These new preparations were highly successful in opacifying the LV cavity and the myocardium from a venous injection. Table 1 lists the various commercially prepared microbubble agents. The 2 currently available in the United States (Definity and Optison) have been approved only for LV cavity opacification. No agents have thus far been approved for myocardial opacification in the United States.

There are salient features common to most of the commercially produced ultrasound contrast agents. The microbubbles in these agents do not aggregate, are biologically inert and safe,[18,19] remain entirely within the vascular space,[20,21] have an intravascular rheology that is very similar to that of erythrocytes,[20–22] respond nonlinearly to ultrasound,[23–25] and are eliminated from the body via the reticuloendothelial system with their gas escaping from the lungs.

A key technical advance in MCE was online signal processing of ultrasound backscatter from insonified microbubbles.[26] Before that, it was not possible to separate bubble signals from myocardial backscatter without offline image processing.[27] Unlike tissue, microbubbles are compressible and oscillate in an ultrasound field. At even a low mechanical index, these oscillations become nonlinear, that is, during each oscillation the microbubbles expand more than they contract. The term *nonlinear* in this context means that the output of a system does not match the input. In other words,

From the Division of Cardiovascular Medicine, Oregon Health and Science University, Portland, Ore.
Correspondence to Sanjiv Kaul, MD, Division of Cardiovascular Medicine, Oregon Health and Science University, UHN62, 3181 SW Sam Jackson Park Rd, Portland, OR 97239. E-mail kauls@ohsu.edu

(*Circulation*. 2008;118:291-308.)

Circulation is available at http://circ.ahajournals.org

DOI: 10.1161/CIRCULATIONAHA.107.747303

Table 1. Ultrasound Contrast Agents

Name	Manufacturer	Shell	Gas	Mean Diameter, μm	Concentration, $\cdot mL^{-1}$	Comments
Levovist	Schering	None; stabilized with 0.1% palmitate	Air	1.2	$1.2–2.0 \cdot 10^8$ when 2.5 g is dissolved in 10 mL saline	Available for cardiological applications in 69 countries but not in the United States
Albunex	Molecular Biosystems, Inc	Denatured human albumin	Air	4.3	$0.5 \cdot 10^9$	Approved for LV cavity opacification in the United States but no longer manufactured
Imagent	Alliance Pharmaceuticals/IMCOR	Surfactant coated	Perfluorohexane	5.0	$0.5 \cdot 10^8$	Approved for LV cavity opacification in the United States but no longer manufactured
Optison	General Electric	Denatured human albumin	Perflutren	3.0–4.5	$5.0–8.0 \cdot 10^8$	Approved for LV cavity opacification in the United States, Europe, and Latin America
Sonazoid	General Electric	Lipid	Perflubutane	2.4–2.5	$0.3 \cdot 10^9$	Approved in Japan for liver opacification
Definity	Lantheus	Lipid	Octafluropropane	1.1–3.3	$1.2 \cdot 10^{10}$	Approved for LV cavity opacification in the United States, Europe, and Latin America and also radiological applications in Canada
Sonovue	Bracco Diagnostics	Lipid	Sulphur hexafluoride	2.5	$5.0 \cdot 10^8$	Available in Europe for LV cavity opacification and radiological applications
Cardiosphere	Point Biomedical, Inc	Bilayer: inner polymer and outer albumin	Nitrogen	3.0	$2.0–5.0 \cdot 10^8$	Under FDA review for MCE
Imagify	Acusphere, Inc	Polymer	Decafluorobutane	2.3	Gas is 260 ± 25 $\mu g \cdot mL^{-1}$ of reconstituted product	Under FDA review for MCE

FDA indicates Food and Drug Administration.

small perturbations can cause large effects.[24,25] With the use of novel signal processing techniques, the nonlinear signals emanating from these oscillating microbubbles can be amplified, and the linear signals can be suppressed, resulting in myocardial opacification.[26] With the use of these approaches, both high–mechanical index intermittent imaging (with the use of B-mode and power Doppler) as well as low–mechanical index continuous imaging are currently being employed for MCE.

The method for assessing (and quantifying) myocardial perfusion during MCE was described and validated in a canine model a decade ago.[28] For this approach, a dilute solution of microbubbles is administered intravenously as a constant infusion with the use of a pump device. In a few minutes, steady state is achieved, at which time the infusion rate can be adjusted depending on the degree of attenuation seen in the LV cavity. Ideally, no shadowing should be seen in the LV cavity on apical views because when shadowing is present, the relation between microbubble concentration in the myocardium and ultrasound backscatter is no longer linear.[28] However, some shadowing should be noted in the left atrium to ensure that there is an adequate concentration of microbubbles in the myocardium at a dose at which the relation between microbubble concentration and backscatter from the LV cavity is still linear. Then high–mechanical index pulses are used to destroy microbubbles in the myocardium, after which their rate of myocardial replenishment is measured. Time versus acoustic intensity (AI) curves can be generated from different myocardial regions and fitted to an exponential function: $y = A(1 - e^{-\beta t})$, where y is AI at a pulsing interval t, A is the plateau AI, and β is the rate constant that represents the rate of rise of AI (and thus mean microbubble velocity).[28]

The unique advantage of this method over other modalities for assessing myocardial perfusion is that it can be used to measure both components of tissue perfusion: myocardial blood flow (MBF) velocity and myocardial blood volume (MBV), the latter being denoted by the value A. Normalizing A to the AI value from the LV cavity provides a measure of MBV fraction.[29] The product of MBV fraction and MBF velocity provides an estimate of MBF. It is preferable to make these measurements with the use of end-systolic frames because at this point in the cardiac cycle most of the larger

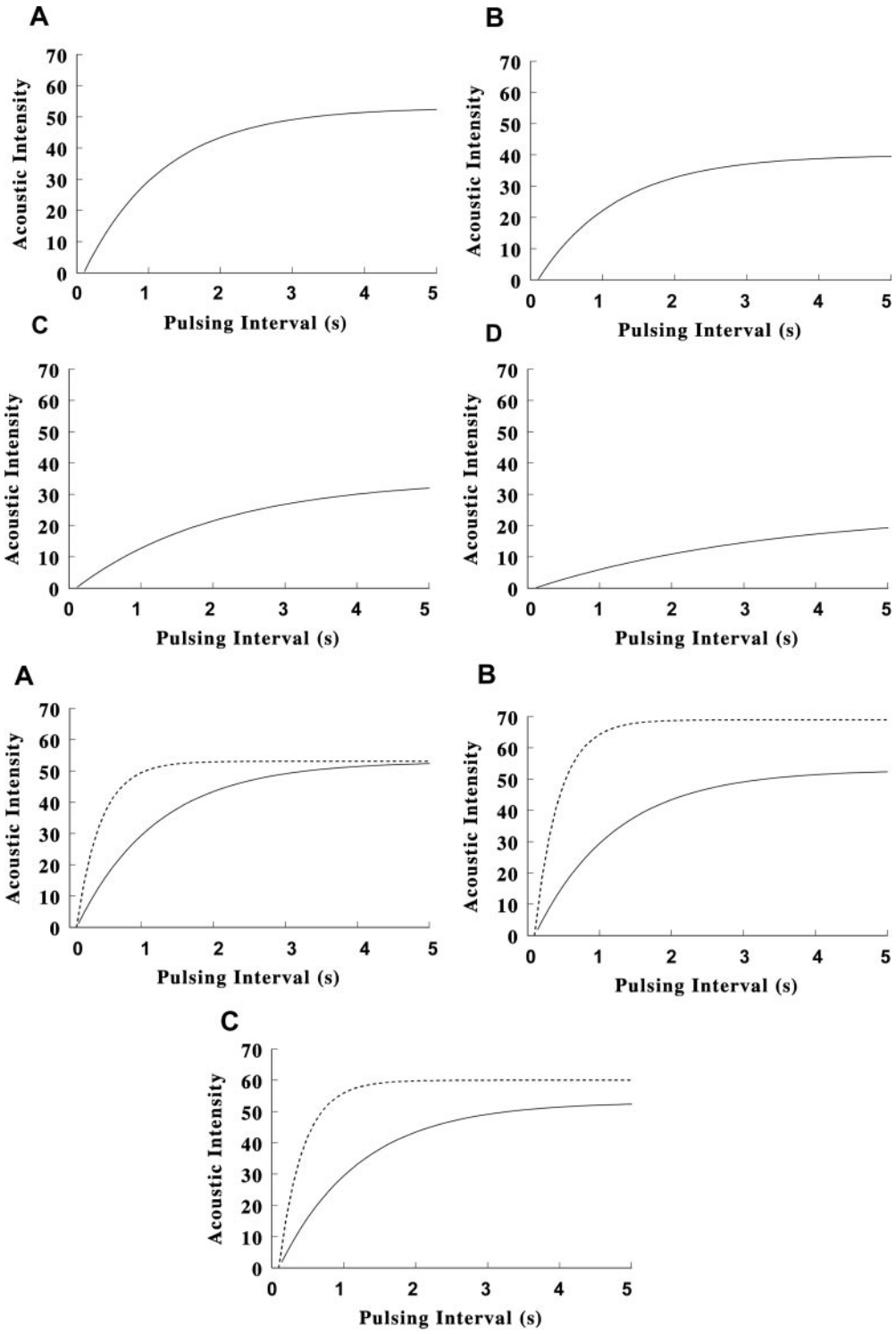

Figure 1. Top, Time vs AI curves obtained at rest from normal myocardium (A), infarcted myocardium supplied by a nonstenotic coronary artery (B), chronically ischemic (hibernating) myocardium (C), and infarcted myocardium supplied by an artery with a flow-limiting stenosis or collaterals (D). See text for details. Bottom, Time vs AI curves obtained at rest (solid line) and stress (dotted line) during intracoronary administration of adenosine (A), during intracoronary administration of dobutamine (B), and during intravenous administration of adenosine or dobutamine (C). See text for details.

intramyocardial vessels have been emptied of blood, and the majority of MBV resides in capillaries, which is the site of nutrient MBF.[30] A modified version of this approach was also validated against positron emission tomography (PET) in humans.[31]

Figure 1 depicts idealized curves based on previous animal and human studies. The top panel of Figure 1 illustrates time versus AI curves that are obtained at rest during normal (Figure 1A [top]) and reduced MBF (Figure 1B to 1D [top]), in which the reduction in MBF can be due to a decrease in

MBV alone (such as after infarction when the infarct-related artery is patent with minimal stenosis; Figure 1B [top]), a decrease in blood velocity alone (such as during subtotal occlusion or total coronary occlusion with collateral flow or hibernating myocardium; Figure 1C [top]), or a combination of both a decrease in MBV and blood velocity such as is seen in an infarcted myocardium supplied either by an artery with a very severe flow-limiting stenosis or by collaterals (Figure 1D). The decrease in MBV in the presence of critical stenosis (Figure 1C [top]) is due to reduced capillary perfusion pressure that results in partial capillary collapse or derecruitment.[32] The more severe the stenosis, the greater is the fall in perfusion pressure, and the greater is the capillary collapse. This changing capillary resistance with decreasing flow is the probable reason for the positive zero-filling coronary pressure.[32] The decrease in capillary blood volume also results in a smaller capillary surface area and a resting perfusion defect on myocardial perfusion imaging with the use of any imaging modality, including nuclear imaging.[33]

The bottom panel of Figure 1 illustrates time versus AI curves obtained from the normal myocardium during rest and different forms of stress. Figure 1A (bottom) depicts curves before and during intracoronary infusion of adenosine in which MBV remains constant and blood flow velocity increases.[28] At rest, the myocardium replenishes in 4 to 5 seconds after microbubble destruction. In the presence of intracoronary adenosine, MBF increases 4 to 5 times solely because of an increase in MBF velocity without any change in MBV. Therefore, instead of taking 4 to 5 seconds to replenish, the myocardium now replenishes in 1 second.

Figure 1B (bottom) shows curves before and during intracoronary infusion of dobutamine (in which both MBV and velocity increase[34]). Figure 1C (bottom) illustrates curves obtained before and during venous administration of either a vasodilator or dobutamine. The increase in MBV during intravenous compared with intracoronary administration of adenosine occurs from the increase in myocardial oxygen demand that results from mild systemic hypotension and resultant reflex tachycardia.[35] Similar curves can also be obtained during supine bicycle exercise.[36]

The comparative efficacy of dobutamine and dipyridamole for coronary stenosis detection was studied in chronically instrumented closed-chest dogs with multivessel coronary stenosis.[37] In the presence of either drug, MBV increased more in the normal bed than in the abnormal bed, but the increase was higher in both beds with dobutamine than it was with dipyridamole. The slope of the relationship between MBF reserve and MBV reserve was greater during administration of dobutamine than with dipyridamole, whereas the converse was true for MBF velocity reserve. Consequently, the relationship of the ratio of either variable between the abnormal and normal beds was similar for both drugs. Thus, these 2 drugs can be used interchangeably for CAD detection by MCE.

MCE in Acute Coronary Syndromes

As stated previously, experimental work in MCE began by establishing its role in defining the presence and size of the risk area during acute coronary occlusion.[4–9] It then progressed to establishing the success of tissue reperfusion as well as the residual infarct size[5,38–41] (via the no-reflow phenomenon), which has been reviewed in great detail previously.[2,3] MCE was used to document the heterogeneity in resting MBF and MBF reserve in the previously occluded bed and the appropriate timing of imaging for determining infarct size.[41–43] Finally, it was used to assess the presence and extent of collateral perfusion during acute coronary occlusion and its influence on myocardial viability.[44–46] These studies were followed by similar ones in humans with the use of intravenous injection of microbubbles.[47–52]

It had been noted for some time that the circumferential extent of abnormal wall thickening overestimated that of infarction. Several mechanisms were postulated to explain this behavior, ranging from mechanical tethering[53] to inherent limitations in the methods of analysis used. With the use of MCE, it has been shown that this disparity is due to collateral-derived intermediate levels of MBF in the border zones of the occluded bed that have escaped necrosis and that the reduction in function in these border zones is commensurate with the reduction in resting MBF.[54]

Recent advances in the management of patients with acute coronary syndromes with MCE pertain to those patients presenting to the emergency department (ED) with chest pain syndromes and nondiagnostic ECGs. In the United States, ≈5 million people visit the ED each year with chest pain. The vast majority is either admitted to the hospital or to a chest pain unit in the ED, but acute myocardial ischemia or infarction (AMI) is confirmed in only ≈20%. The initial ECG is diagnostic in fewer than half of the patients with ongoing AMI, and cardiac enzymes do not become positive for several hours after coronary occlusion. Meanwhile, valuable time is lost before definitive therapy can be offered.

A multicenter study compared MCE with single photon emission computed tomography (SPECT) to diagnose AMI in chest pain patients with a nondiagnostic ECG.[55] Concordance between MCE and SPECT was 77% for all territories with a higher concordance for the anterior wall (84%). Thirty-eight of the 203 patients in the study (19%) had a cardiac event within 48 hours of ED presentation. On multivariate regression analysis, the number of abnormal segments on MCE and SPECT was a significant predictor of cardiac events. MCE provided 17% and gated SPECT provided 23% additional information for predicting cardiac events compared with routine demographic, clinical, and ECG variables that were available in the ED at the time of presentation. Another smaller single-center study also reported similar results.[56]

A large National Institutes of Health–funded single-center study showed even more remarkable results.[57] Of the 1017 patients studied, 166 (16.3%) had early (within 48 hours) events. Adding regional function assessment by MCE increased the prognostic information of the clinical and ECG variables significantly for predicting these events. When myocardial perfusion assessment was added, further additional information was obtained (Figure 2A). Patients without early events were followed for a median of 7.7 months. Of these, 126 had events. The added prognostic value of both regional function and myocardial perfusion assessments on MCE was similar to that seen for the early events. Patients

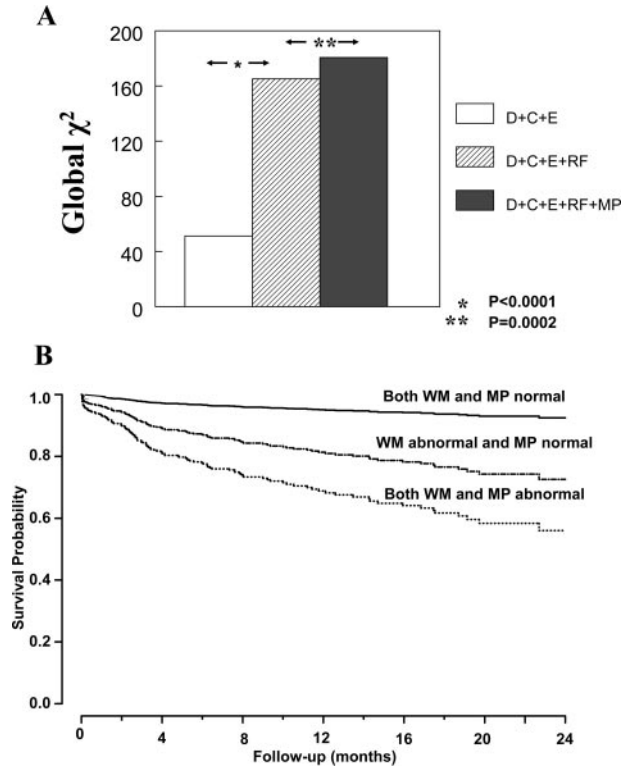

Figure 2. A, Incremental value of tests performed for prediction of early events in patients with nondiagnostic ECGs undergoing ED evaluation for chest pain.[57] D indicates demographics; C, clinical; E, ECG; RF, regional function; and MP, myocardial perfusion. See text for details. With permission from the European Society of Cardiology. B, Adjusted survival probabilities for different combinations of regional function and myocardial perfusion values for late events (occurring after 48 hours) in patients presenting to the ED with nondiagnostic ECGs. WM indicates wall motion. See text for details. Modified from Rinkevich et al,[57] with permission. Copyright 2005, Oxford Journals Press.

with normal perfusion and function had excellent outcome, whereas those in whom both were abnormal had the worst outcome. Intermediate outcome was noted in those with normal perfusion despite abnormal function (Figure 2B). These patients included those with spontaneous reperfusion (approximately one sixth of the AMI patients) and those with nonischemic cardiomyopathies.

Although an elevated troponin level is the gold standard for AMI diagnosis, it may not be elevated or even available at the time of ED presentation. It is at this juncture that MCE has been shown to be most helpful.[58] In this study, a modified Thrombolysis in Myocardial Infarction (TIMI) score was calculated from 6 immediately available variables, which did not include troponin because it was not known at that time. Follow-up was performed for early (within 24 hours), intermediate (30 days), and late (after 30 days) events. The modified TIMI score was unable to discriminate between intermediate-risk compared with high-risk patients at any follow-up time point, whereas only 2 of 523 patients with normal regional function on MCE had an early event. Regional function on MCE provided incremental information over modified TIMI scores for predicting intermediate and late events. In patients with abnormal regional function, myocardial perfusion further classified those into intermediate- and high-risk groups. The full TMI score (after troponin levels became available) could not improve on these results at any follow-up time point. Since this study was completed, another ≈1000 patients have been analyzed, and, interestingly, multivariate models derived from the first 1000 patients predict early events in these patients with the same accuracy.

On the basis of the results of these studies, 2 separate editorials have strongly recommended the use of MCE in the ED.[59,60]

Figure 3A illustrates a case of Tako-Tsubo syndrome in which apical ballooning (arrows) is clearly seen in the end-systolic image, but myocardial perfusion is normal. On the basis of this study in the ED, the patient was not taken to the catheterization laboratory, and the regional dysfunction resolved spontaneously. Although Tako-Tsubo syndrome may be associated with microvascular abnormalities, these may be subtle and occur early in the pathogenesis of the syndrome. Generally, by the time MCE is performed, myocardial perfusion is normal.[61] Figure 3B shows a patient examined in the ED for chest pain who not only had an apical defect on MCE (thick arrow) but very nicely demonstrated an apical thrombus as well (thin arrow). Contrast echocardiography has become the gold standard for detecting LV cavity thrombi, which has obvious implications for therapy.

MCE for CAD Detection

In the absence of prior infarction, the detection of CAD on myocardial perfusion imaging is based on the occurrence of

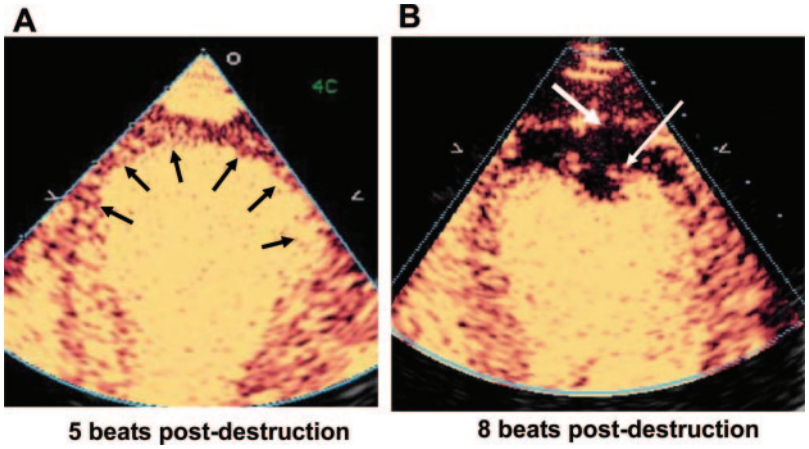

Figure 3. A, Low–mechanical index real-time MCE showing normal perfusion in a patient with apical ballooning (arrows) who was seen in the ED for chest pain. B, Low–mechanical index real-time MCE showing a dense apical defect in a patient with chest pain who experienced an AMI (thick arrow). An apical thrombus is also noted (thin arrow).

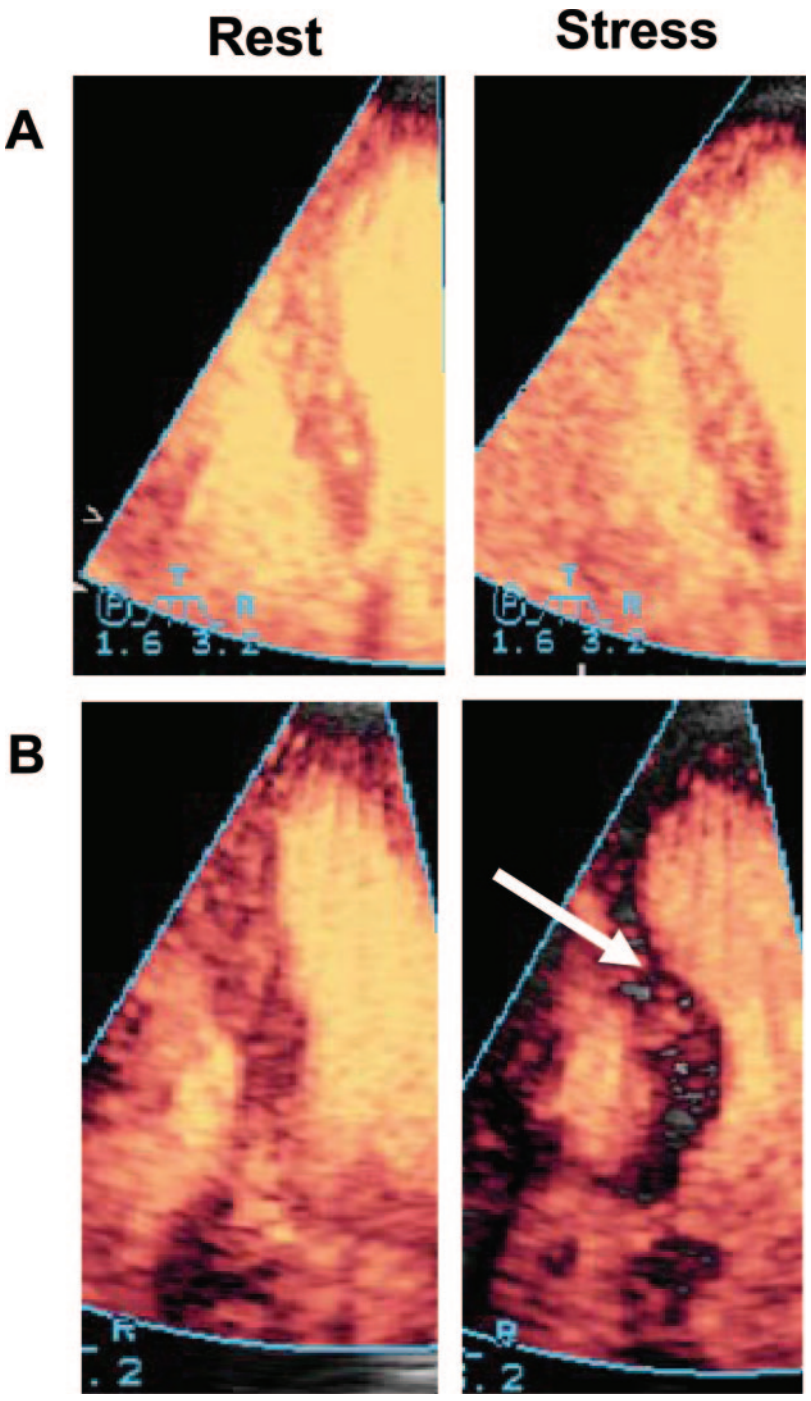

Figure 4. A, High–mechanical index intermittent power Doppler images obtained at rest and stress showing normal myocardial perfusion. See text for details. B, High–mechanical index intermittent power Doppler images obtained at rest and stress showing a reversible defect (arrow). See text for details.

reversible perfusion defects during pharmacological or exercise stress. Experimental studies had previously demonstrated the ability of MCE to detect coronary stenosis and to quantify the degree of MBF mismatch during pharmacological stress.[62–64] Studies also showed that coronary stenosis can be detected[65,66] and abnormal coronary blood flow reserve can be accurately measured[67] with MCE in humans with venous administration of microbubbles.

The conventional wisdom had been that a reversible perfusion defect results from MBF mismatch that is seen at stress and not at rest. With the use of MCE, it has been shown that reversible perfusion defects are actually caused by a decrease in MBV distal to a stenosis during stress.[32] When flow increases through a stenosis during stress, the coronary perfusion pressure falls. To maintain a constant capillary hydrostatic pressure, capillary derecruitment occurs, leading to a decrease in MBV. In the case of nuclear tracers, the resultant decrease in capillary surface area causes less tracer uptake and hence a perfusion defect.[33] Thus, the site of abnormal flow reserve in CAD is not at the level of the stenosis but actually at the level of the microcirculation.

The decrease in MBV during stress is seen only with moderate to severe stenosis. With less severe stenosis, the only abnormality seen on MCE is the inability of the MBF

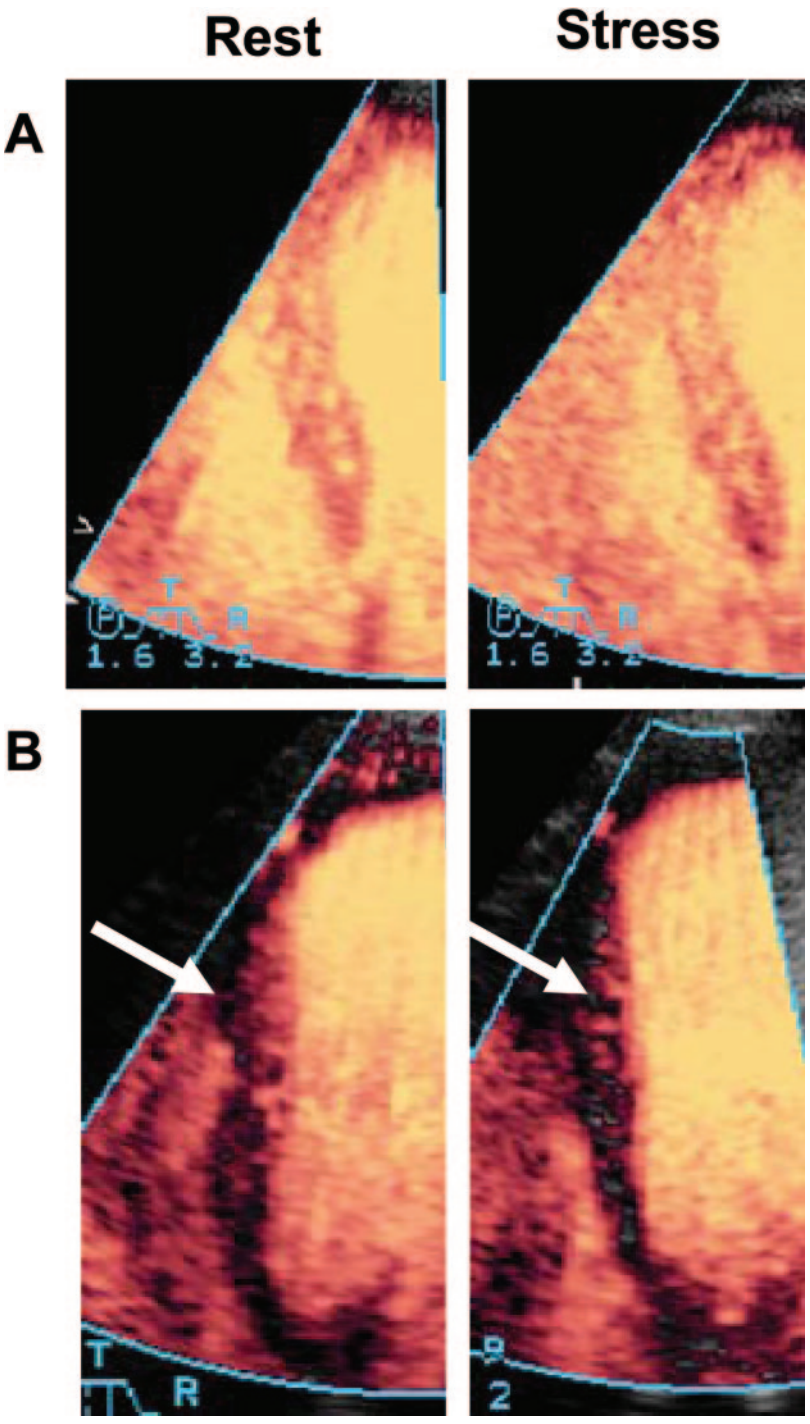

Figure 5. A, High–mechanical index intermittent power Doppler images obtained at rest and stress showing normal myocardial perfusion. See text for details. B, High–mechanical index intermittent power Doppler images obtained at rest and stress showing a fixed defect (arrow). See text for details.

velocity to increase by the desired amount. As shown in the bottom panel of Figure 1, MBF velocity increases 4 to 5 times in the normal myocardium during stress. The inability of the MBF velocity to increase by this amount during stress indicates a reduction in MBF reserve. What discriminates the attenuation of flow reserve in the presence of a stenosis compared with other causes such as hypertrophy, and hyperlipidemia is its regional nature.[67]

Figures 4 and 5 demonstrate normal perfusion (top panels) and either a reversible (Figure 4) or a fixed (Figure 5) defect (bottom panels) in patients undergoing dipyridamole stress imaging with the use of Cardiosphere. The imaging protocol is based on the principles depicted in the bottom panel in Figure 1. At rest, microbubble replenishment should occur in 4 to 5 seconds if MBF is normal. Therefore, the rest images (left panels) are captured at the fourth heartbeat after bubble destruction. If MBF reserve is normal, then at stress the myocardium should replenish within 1 second. Hence, the stress images are captured at the first heartbeat after bubble destruction (right panels). In the normal setting, these 2 images (rest and stress) should look similar (panel A in both figures). If there is a significant stenosis in the absence of prior infarction, the stress image should show a relative defect compared with the rest image (indicated by arrows in Figure

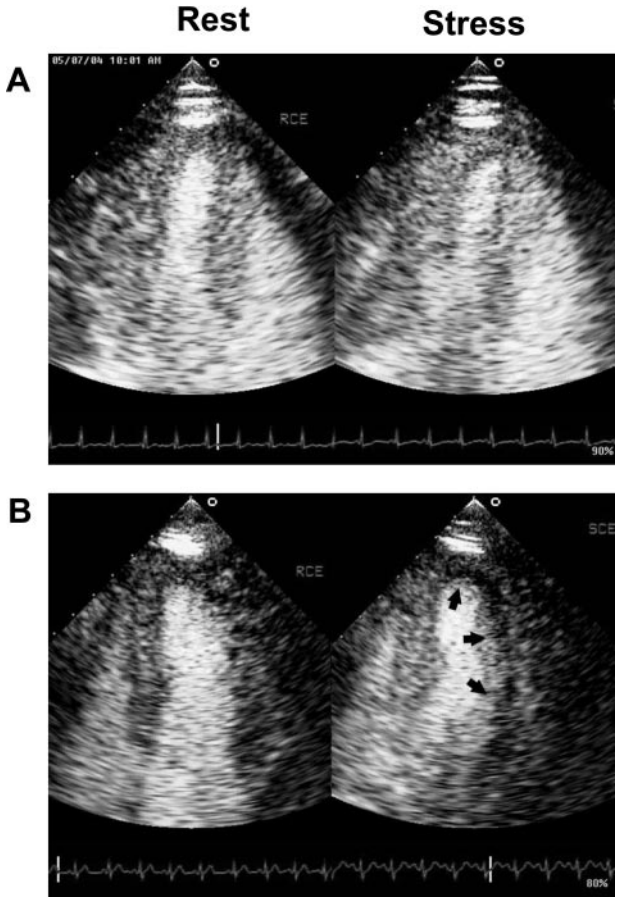

Figure 6. A, Low–mechanical index real-time images obtained at rest and stress showing normal myocardial perfusion. See text for details. B, Low–mechanical index real-time images obtained at rest and stress showing a reversible defect (arrow). See text for details.

4B). In the presence of infarction, in which MBV is markedly reduced due to capillary loss, a fixed defect (present at both rest and stress) should be noted (indicated by arrows in Figure 5B). The images shown here were obtained with the use of power Doppler, with each wall in each view imaged separately because of the narrow imaging sector necessary for a high-pulse repetition frequency required to minimize motion artifacts.

Figure 6 illustrates rest and stress (dipyridamole) images obtained with the use of Imagify. Here the images are acquired with the use of real-time low–mechanical index imaging. Figure 6A depicts a normal study, whereas Figure 6B depicts a reversible lateral defect (denoted by arrows) in a patient with a proximal left circumflex artery stenosis. In this particular case, the nuclear scan was entirely normal.

The top panel in Figure 7 depicts MCE and SPECT results from a multicenter study of 55 patients with an intermediate probability of CAD who did not have a prior infarction.[68] Thus, their resting function and perfusion were normal. From a clinical perspective, it is in these patients that the ability to diagnose CAD is most relevant. It is evident from the top panel in Figure 7 that the sensitivity of MCE was higher than that of SPECT at mild to moderate levels of stenosis. This occurred because abnormalities in MBF velocity were noted on MCE even when MBV may not have decreased (see bottom panel in Figure 7 and later discussion), resulting in abnormal MCE images but a normal stress SPECT study. Only at severe levels of stenosis, in which MBV reduction is almost certain to occur during hyperemia, was SPECT equivalent to MCE. Another reason for the superiority of MCE over SPECT for detecting mild to moderate stenoses was the presence of subendocardial perfusion defects on the former that could not be visualized on the latter because of the poor spatial resolution of SPECT.

On a coronary circulation basis (anterior and posterior myocardium), the sensitivity for MCE in this study was significantly higher than that of SPECT for the detection of CAD (86% versus 43%). The specificities of MCE and SPECT, however, were similar (88% and 93%). Both techniques were marginally more accurate in the anterior compared with the posterior circulation. On a patient basis, MCE had a higher sensitivity than SPECT for the detection of CAD (83% versus 49%), although specificity tended to be higher for SPECT than MCE (92% versus 58%). When CAD was defined as >40% rather than >50% coronary stenosis on quantitative coronary angiography, the specificity of MCE increased to 83% without any change in sensitivity.

Several other small studies have compared MCE with SPECT during vasodilator stress,[69] and some others have been summarized in a meta-analysis showing an overall superiority of MCE to SPECT.[70] More recently, the results of 2 large (a total of 662 patients from 28 centers) phase III clinical trials performed to determine the efficacy of Imagify for detecting CAD in patients with chronic stable chest pain demonstrated a similar performance for MCE and SPECT.[71] Interestingly, in this study wall motion abnormality on dipyridamole stress was much more frequent than reported previously in literature published in the United States. Most probably this resulted from a much better assessment of regional function with contrast in the LV cavity. Because in most instances even low-dose dipyridamole ($0.56\ mg \cdot kg^{-1}$) causes some degree of hypotension and reflex tachycardia, an increase in myocardial oxygen consumption is frequent, which can explain the occurrence of wall motion abnormalities,[72,73] that are much better appreciated when contrast is present in the LV cavity.

The ischemic cascade had been demonstrated previously in supply but not demand ischemia.[74] This phenomenon was more recently demonstrated in demand ischemia as well with the use of MCE.[75] It was shown that in the presence of noncritical coronary stenosis, perfusion abnormalities occurred earlier than wall motion abnormalities with escalating doses of dobutamine. Abnormal perfusion (delayed rate of microbubble replenishment) was seen at the lowest dose of dobutamine irrespective of the stenosis severity, whereas wall thickening abnormality was seen only at high doses of dobutamine and was influenced by the stenosis severity. The bottom panel of Figure 7 illustrates an example of normal wall thickening (Figure 7A) despite abnormal perfusion (denoted by arrows in Figure 7B) in an animal with left circumflex artery stenosis during dobutamine infusion. Figure 7C depicts the time versus AI curves, showing delayed filling in the left circumflex coronary artery bed. In this study, even

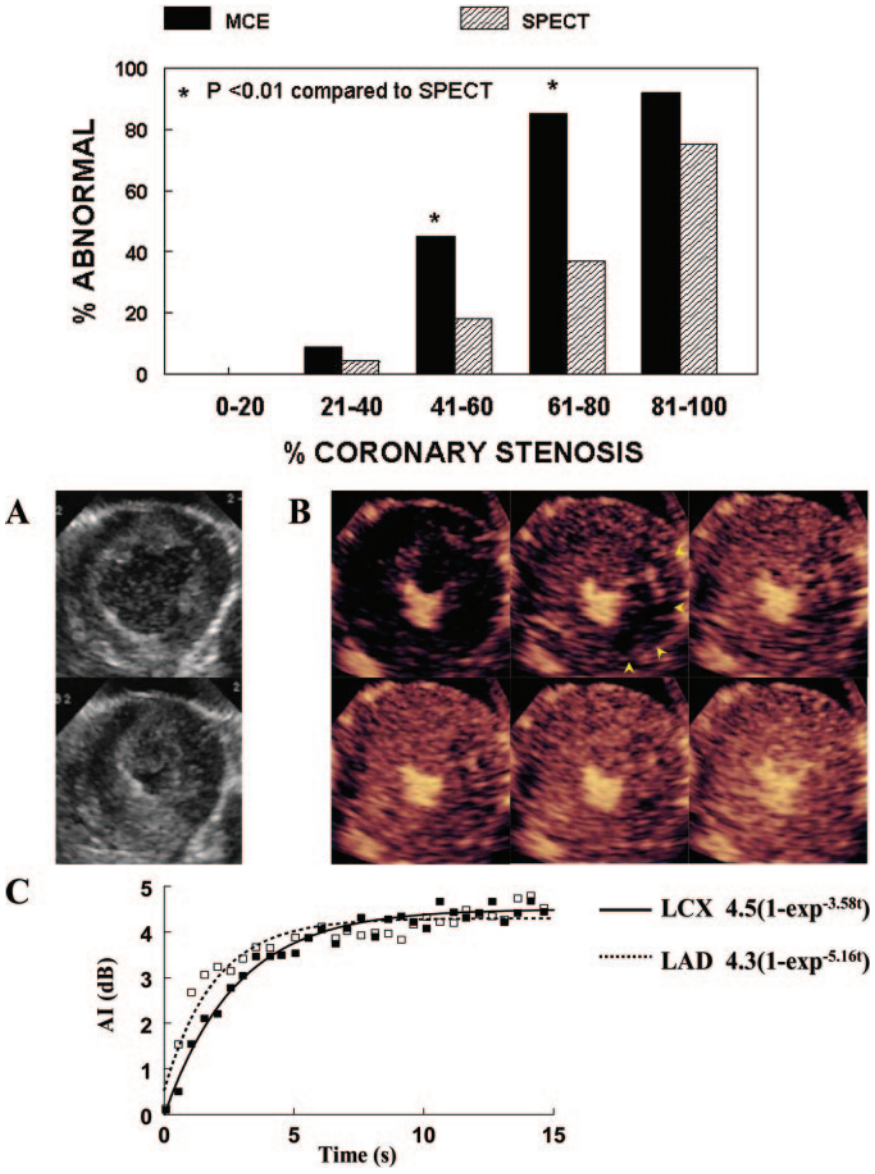

Figure 7. Top, Comparison of perfusion defect occurrence on MCE and SPECT during dipyridamole stress imaging based on the degree of coronary stenosis determined by quantitative coronary angiography. See text for details. Reprinted from Senior et al,[68] with permission from Elsevier. Bottom, Images from a dog with a moderate left circumflex stenosis during 10 $\mu g \cdot kg^{-1} \cdot min^{-1}$ of dobutamine. A, End-diastolic and end-systolic images with normal wall thickening. B, MCE frames at different time points after microbubble destruction showing slow left circumflex bed filling. C, Time vs AI curves showing slower filling in the left circumflex (LCX) compared with the left anterior descending (LAD) artery bed. Reprinted from Leong-Poi et al,[75] with permission from Lippincott Williams & Wilkins. Copyright 2002, American Heart Association.

when wall thickening abnormality occurred in single-vessel stenosis, it was less in extent than the perfusion defect.

Another series of experiments demonstrated that the mechanism of the disparity in the circumferential extent of abnormal wall thickening and perfusion defect during demand ischemia (the former being significantly less than the latter) was due to the presence of collateral MBF in the border zones of the ischemic bed.[54] It was shown that at higher levels of MBF (>3 times normal), the relation between MBF and wall thickening was flat (Figure 8A). Thus, regions at the borders supplied with collateral flow that did not experience as much hyperemia as the remote normal beds nonetheless continued to exhibit as much thickening.

These principles were confirmed in clinical reports. In 1 study, 170 patients underwent dobutamine-atropine stress testing.[76] The sensitivity of MCE was higher than that of wall motion at both maximal (91% versus 70%) and intermediate (84% versus 20%) doses of dobutamine. Specificity was lower for MCE compared with wall motion abnormality (51% versus 74%). Most of the perfusion defects occurred at intermediate levels of stress when side effects of dobutamine were minimal. Similar results were subsequently reported in patients with diabetes, a high-risk group in whom CAD detection is very important.[77]

In a retrospective analysis, 788 patients undergoing dobutamine stress were followed up for a median of 20 months. It was shown that myocardial perfusion assessment on MCE had significant incremental value over clinical factors, resting ejection fraction, and wall motion responses in predicting events.[78] As shown in Figure 8B, the 3-year event-free survival was 95% for patients with normal perfusion and function, 82% for those with normal function but abnormal perfusion, and 68% for those with both abnormal function and perfusion. When these data are interpreted on the basis of results of previous experimental studies, it likely that patients with both abnormal perfusion and function have a higher incidence of multivessel CAD and compromised collateral perfusion. Similar results have been reported in elderly

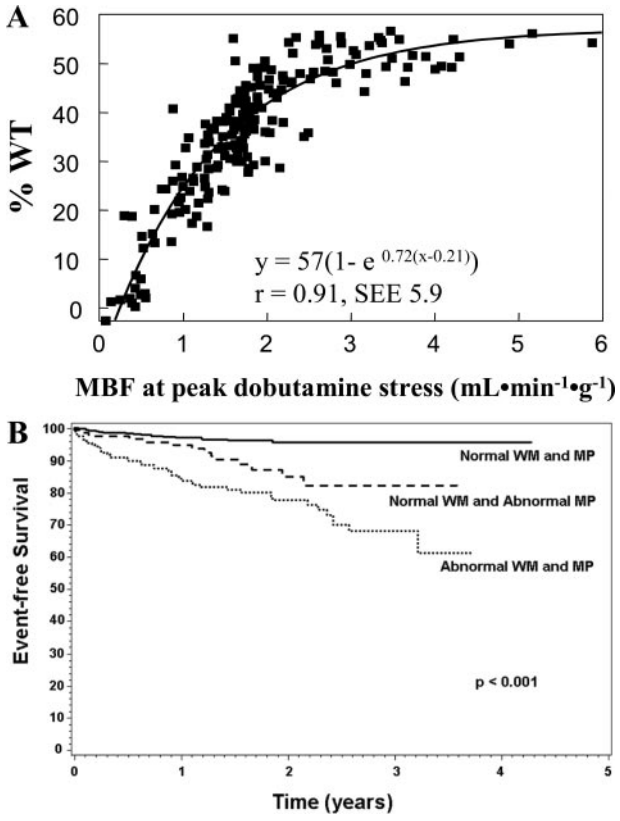

Figure 8. Top, Relation between radiolabeled microsphere–derived MBF and wall thickening (WT) during dobutamine infusion. As MBF increases from 0 to 3 mL · g^{-1} · min^{-1}, WT also increases. However, at >3 mL · g^{-1} · min^{-1}, WT remains flat. See text for details. Reprinted from Leong-Poi et al,[54] with permission from Elsevier. Copyright 2005, American College of Cardiology. Bottom, Long-term outcome in patients undergoing dobutamine-atropine stress testing based on the combination of wall motion (WM) and myocardial perfusion (MP).See text for details. Reprinted from Tsutsui et al,[78] with permission from Lippincott Williams & Wilkins. Copyright 2005, American Heart Association.

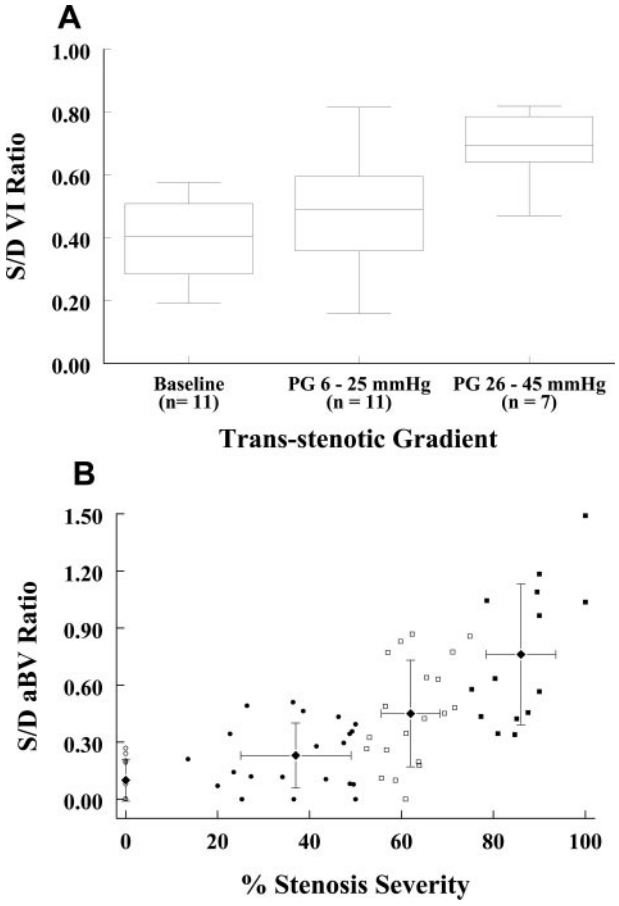

Figure 9. A, Systolic (S) vs diastolic (D) video intensity (VI) ratios obtained in dogs with increasing levels of coronary stenosis and normal MBF (noncritical stenoses). See text for details. Reprinted from Wei et al,[84] with permission from Lippincott Williams & Wilkins. Copyright 2002, American Heart Association. B, Systolic (S) vs diastolic (D) aBV ratio in patients with different degrees of coronary stenosis based on quantitative coronary angiography. PG indicates pressure gradient. See text for details. Modified from Wei et al,[85] with permission from Lippincott Williams & Wilkins.

patients[79] as well as in those with diabetes[80,81] and advanced liver disease.[82]

As stated earlier, in the current practice of cardiology, some form of stress is required to detect CAD on myocardial perfusion imaging. Unless there is a previous infarction, resting perfusion remains normal despite the presence of up to 85% luminal diameter narrowing of the coronary artery because of autoregulation. In the presence of a noncritical stenosis, autoregulation causes an increase in total coronary blood volume (volume of blood in the entire coronary tree), primarily from enhanced dimensions of arterioles.[83]

Because the blood in myocardial arterioles comprises only a small proportion of MBV, microbubble signals from these vessels are usually negligible when the ultrasound beam is fully replenished after microbubble destruction. However, if imaging is performed with a very short interval between destructive ultrasound pulses, the signal obtained is derived only from vessels that fill in this short period of time, as neither capillaries nor venules have adequate time to fill.[84,85] Thus, this approach can be used to image the blood volume of relatively larger intramyocardial vessels.

During systole, a change in myocardial elastance causes retrograde displacement of the arteriolar blood volume (aBV) into the larger intramyocardial arterioles, resulting in a small systolic signal from these vessels on MCE. In the presence of a stenosis, because aBV is larger as a result of autoregulation, greater retrograde displacement of microbubbles from smaller arterioles into the larger intramyocardial arterioles occurs, resulting in an increase in the systolic myocardial signal from these vessels. Because the larger intramyocardial arterioles do not participate in autoregulation, the diastolic signal from them remains unchanged. It was first shown in an animal model[84] (Figure 9A) and then in humans[85] (Figure 9B) that the systolic-to-diastolic aBV signal ratio measured at rest increases in the presence of a noncritical stenosis and that the degree of increase is proportional to coronary stenosis severity. Thus, by exploiting the microcirculatory compensatory mechanisms that are evoked to maintain a constant perfusion pressure distal to a stenosis, we can detect the presence of stenosis even at rest using a novel adaptation of MCE.[86]

As can be seen from Figure 9B, a normal systolic-to-diastolic aBV ratio can sometimes be seen even in the presence

of moderate to severe coronary stenosis. It was hypothesized that this is caused by collateral blood flow. In a canine model of coronary stenosis, measurements were made in collateralized and noncollateralized myocardium. The systolic-to-diastolic aBV signal ratio in the noncollateralized bed increased significantly with increasing stenosis severity, whereas in the collateralized bed it did not.[87] Because extensive collateralization may indicate excellent prognosis, this ratio may provide a more appropriate assessment of the myocardium despite the presence of significant coronary artery stenosis and hence better prognostic information than that provided by the coronary anatomy.

MCE for Detecting Viability in Chronic CAD

One of the earliest experimental and clinical applications for MCE was the detection of myocardial viability based on microcirculatory integrity after attempted reperfusion in AMI.[5,38–43,47–49] Another aspect was the maintenance of myocardial viability in AMI based on adequate collateral MBF.[44–46] More recently, attention has shifted to the assessment of viability in chronic CAD. MCE was compared with ^{201}Tl imaging and low-dose dobutamine stress in patients with CAD and dysfunctional myocardium undergoing coronary bypass surgery.[88] It was found that the sensitivity of MCE for recovery of function after bypass was 90% and was similar to that of ^{201}Tl imaging (92%) and dobutamine echocardiography (80%). However, the specificity of MCE was higher (63%) than that of the other 2 techniques (45% and 54%). These patients also underwent myocardial biopsies during bypass surgery to correlate MCE parameters to histology.[89] As expected, MBV ratios from different beds correlated very well with microvascular density and capillary area ratios from these beds (r=0.84 and r=0.87, respectively). Also not surprisingly, MCE-derived MBF was a better predictor of functional recovery than MBV alone.

Another study examined patients presenting with acute heart failure who had no previous infarction or history of CAD.[90] Clinically, in these patients 2 questions need to be answered. Do they have CAD, and if they do, is the myocardium viable? In this study, the sensitivity, specificity, and positive and negative predictive values of stress MCE for the detection of CAD were 82%, 97%, 95%, and 88%, respectively. Quantitative MCE demonstrated significantly lower MBF velocity reserve in patients with CAD compared with those with normal coronary arteries. Almost all patients with CAD had reversible defects indicating the presence of viable myocardium. Thus, MCE was able to answer the 2 critical questions at the bedside without requiring a more cumbersome assessment through SPECT, PET, or magnetic resonance imaging.

MCE for Site-Targeted Imaging

As stated earlier, microbubbles used for MCE have a rheology that is similar to that of erythrocytes.[20–22] Therefore, it was unexpected when instead of flowing freely through tissue, microbubbles were found to be sticking in the myocardium after cold crystalline cardioplegia delivery both in animal models[91] and in humans.[92] This sticking was not related to any of the cardioplegia constituents (including oxygen content) or temperature and was not seen when the myocardium was reperfused by venous rather than arterial blood,[93] in which free oxygen radical–induced injury is less. Similar microbubble sticking was noted during ischemia/reperfusion, and it was found that the microbubbles were in fact adhering to activated leukocytes via cell-surface integrins or complement-mediated opsonization depending on the microbubble used.[94] Thus began the journey with site-targeted (or molecular) imaging with MCE.

Table 2. Targets for Microbubble-Based Molecular Imaging Pertaining to the Cardiovascular System

Molecule Targeted	Pathophysiological Substrate	Experimental Conditions in Which Shown to be Successful
Phosphatidyl serine	Activated leukocytes, inflammation	Ischemia/reperfusion injury[94,100–102]
ICAM-1	Inflammation	Activated endothelial cells[98]
		Cardiac transplant rejection[99]
VCAM-1	Inflammation	Early atherosclerosis[107]
P-selectin	Inflammation	Ischemic memory[106]
Sialyl Lewis	Inflammation	Ischemic memory[105]
αV-integrins	Angiogenesis	Tumor angiogenesis[96]
		Angiogenesis in hindlimb ischemia[95]
Arg-Arg-Leu	Angiogenesis	Tumor angiogenesis[97]
Glycoprotein IIb/IIIa	Activated platelets	Microthrombosis[103]

ICAM-1 indicates intracellular adhesion molecule-1; VCAM-1, vascular cell adhesion molecule-1.

The advantage of MCE over modalities such as magnetic resonance imaging is that because of their nonlinear behavior when exposed to ultrasound, very few bubbles need to be present in the target to produce signal. Therefore, the signal-to-noise ratio is very good. The disadvantage that MCE has over other modalities, especially PET/CT, is that targets limited only within the vascular space can be imaged. Table 2 lists the targets that have been imaged successfully with MCE with the use of either antibodies or small molecules and the different experimental conditions in which they have been shown to be useful. Many of these applications are outside the heart or even the cardiovascular system.

In terms of the myocardium, the obvious potential applications of this approach are imaging of angiogenesis (especially in the context of cell and gene therapy)[95–97]; acute and chronic cardiac transplant rejection (in which it could supplant the more invasive cardiac biopsies)[98,99]; ischemia/reperfusion injury, especially if one can modulate it (see later)[94,100–102]; imaging microthromboembolism during percutaneous coronary interventions (to determine effective therapy for the no-reflow phenomenon)[103,104]; and ischemic memory (to differentiate new from old wall motion abnormality in the setting of chest pain).[105,106] Early coronary atherosclerosis can also be detected with this approach.[107] Microbubbles can also bind to early atherosclerotic lesions nonspecifically by complement-mediated adhesion.[108]

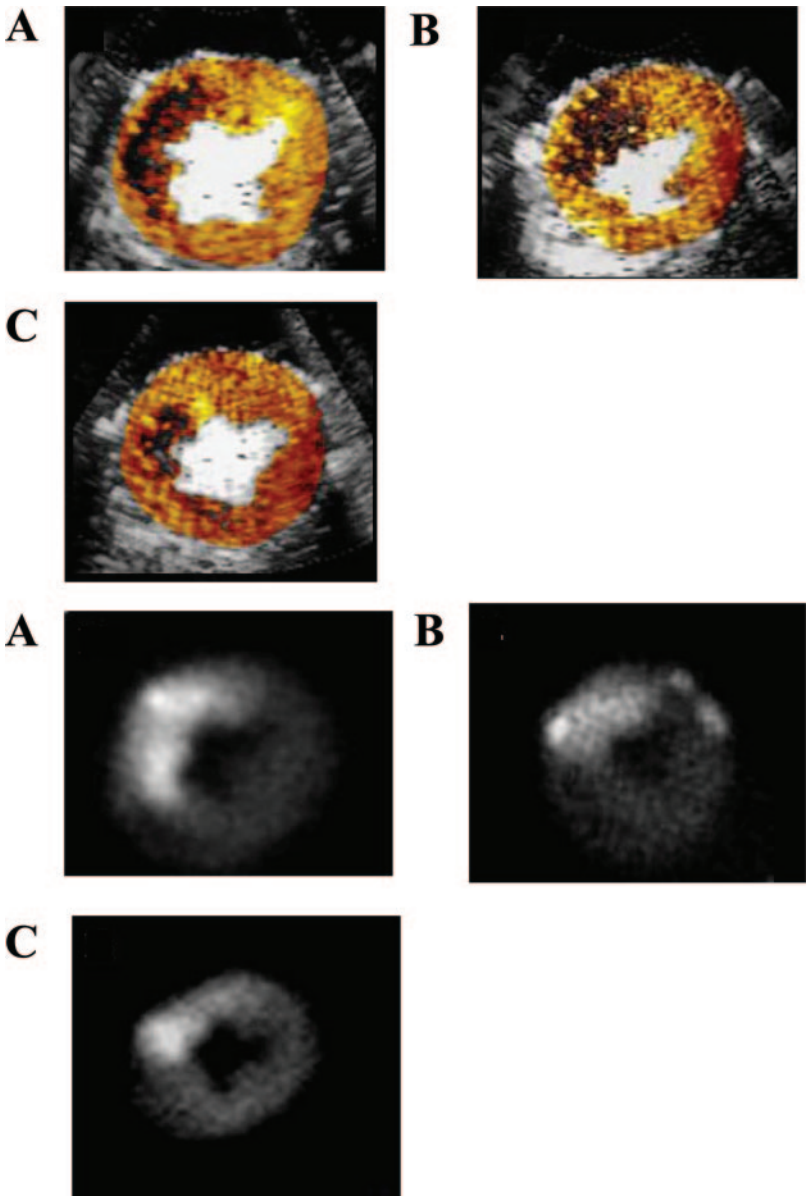

Figure 10. Top, MCE-derived no-reflow images from dogs receiving saline (A) (group 1), tirofiban (B) (group 2), and CP-4715 (C) (group 3). See text for details. Reprinted from Sakuma et al,[109] with permission of the European Society of Cardiology. Bottom, Platelet aggregation in the myocardium 180 minutes after recanalization on ^{99m}Tc-DMP-444 autoradiography. A, B, and C are same as in top panel. See text for details. Reprinted from Sakuma et al,[109] with permission of the European Society of Cardiology.

Described herein is an experiment in which MCE-based molecular imaging was used to determine the efficacy of therapy aimed at reducing infarct size in a setting of percutaneous coronary intervention performed for acute coronary thrombosis. The reason to present these results is to indicate possible ways in which molecular imaging could be used to determine the effect of treatments.

The thrombus burden influences the size of the no-reflow phenomenon as well as infarct size after attempted coronary intervention,[104] suggesting that the beneficial effects of platelet glycoprotein IIb/IIIa receptor blockade may be due in part to reduction in microthromboemboli. Another consequence of ischemia/reperfusion is endothelial activation from oxygen free radicals and tissue factor, resulting in the expression of the $\alpha_{v\beta3}$, which, in turn, causes platelets to adhere to the endothelium. In the presence of microthromboemboli, prothrombin can bind to both IIb/IIIa and $\alpha_{v\beta3}$, resulting in additional thrombus formation. Activation of $\alpha_{v\beta3}$ is also associated with leukocyte entrapment within the platelet-fibrin mesh as well as monocyte adhesion to the endothelium. These effects could reduce microvascular perfusion and cause more ischemia.

Thus, the therapeutic aim of this experiment was the combined inhibition of $\alpha_{v\beta3}$ and IIb/IIIa with the use of a novel synthetic compound, CP-4715, whose action was compared with that of tirofiban, which predominantly blocks the IIb/IIIa receptor.[109] A control group (saline) was also used. Myocardial activities of $\alpha_{v\beta3}$ and IIb/IIIa were measured with echistatin-labeled microbubbles[95] and ^{99m}Tc-labeled DMP-444,[104] respectively. Inflammation was assessed with phosphatidyl serine–coated microbubbles.[102]

Whereas the risk area size was similar between the 3 groups, the no-reflow zone was different, as demonstrated by the examples shown in the top panel of Figure 10. It was the largest in the group 1 dog receiving saline (Figure 10A [top]), intermediate in the group 2 dog receiving tirofiban (Figure

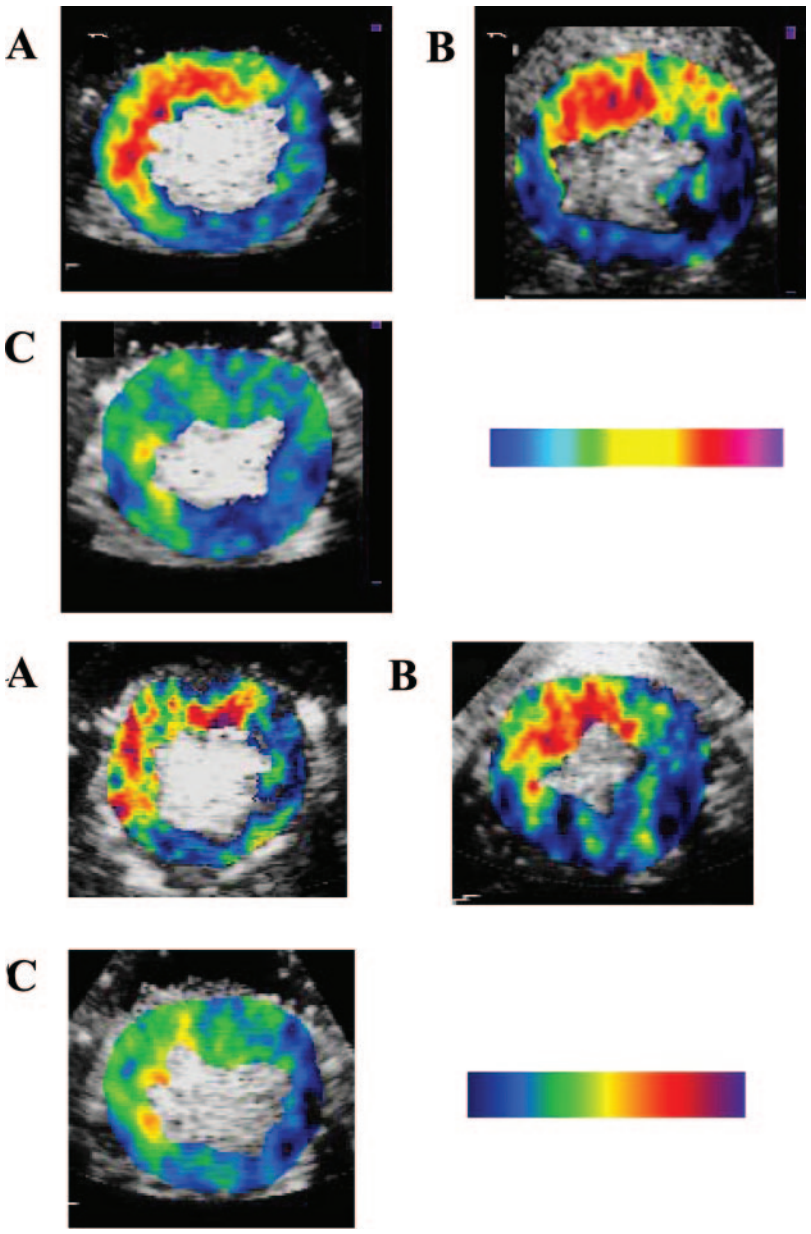

Figure 11. Top, Myocardial $\alpha_{v\beta3}$ activity measured with the use of backscatter from echistatin-conjugated microbubbles. A, B, and C are same as in Figure 10, top panel. See text for details. Reprinted from Sakuma et al,[109] with permission of the European Society of Cardiology. Bottom, "Inflammation" imaging from phosphatidyl serine–conjugated microbubbles. A, B, and C are same as in Figure 10, top panel. See text for details. Reprinted from Sakuma et al,[109] with permission of the European Society of Cardiology.

10B [top]), and smallest in the group 3 dog receiving CP-4715 (Figure 10C [top]). ^{99m}Tc-DMP-444 activity on autoradiography is shown in the bottom panel in Figure 10. It was higher in group 1 (Figure 10A [bottom]) compared with group 2 and 3 dogs (Figure 10B and 10C [bottom]), indicating some reduction in microthromboemboli with IIb/IIIa inhibition caused by both drugs. Background-subtracted color-coded images after administration of echistatin-conjugated microbubbles are shown in the top panel in Figure 11. There was the least backscatter in group 3 dogs (Figure 11C [top]), indicating effective inhibition of $\alpha_{v\beta3}$ by CP-4715. Similar images after administration of phosphatidyl serine–coated microbubbles are shown in the bottom panel of Figure 11. The backscatter was the lowest in the group 3 dogs (Figure 11C [bottom]), indicating suppression of inflammation by CP-4715. Overall, there was a 59% reduction in infarct size in the group 3 dogs receiving CP-4715 compared with controls and a 37% reduction compared with the group 2 dogs receiving tirofiban. Thus, the combined suppression of both IIb/IIIa and $\alpha_{v\beta3}$ markedly limits no-reflow and tissue injury.[109]

Miscellaneous Applications and Findings

MCE has been found to be very effective in identifying the septal perforator arteries that supply the thickened muscle, which contributes to outflow track obstruction in hypertropic cardiomyopathy. Thus, selective intracoronary injections of microbubbles can be used to define the vessel through which alcohol needs to be administered for creating localized necrosis and reduction in the outflow tract gradient.[110] MCE has also been used for visualization of the right ventricular myocardium[111] and to demonstrate improved perfusion after stem cell therapy.[112] A particularly innovative application has been in the evaluation of cardiac tumors. Malignant tumors

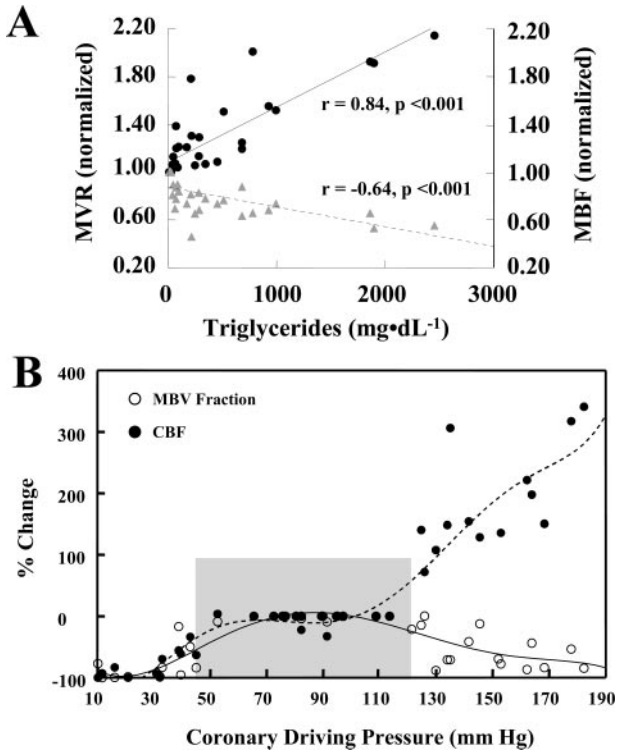

Figure 12. A, Effect of serum triglyceride levels (*x* axis) on myocardial vascular resistance (MVR, left *y* axis; filled circles) as well as radiolabeled microsphere–derived MBF (right *y* axis; triangles) in the presence of maximal hyperemia. All values are normalized to baseline hyperemic values in each dog. See text for details. Reprinted from Rim et al,[118] with permission from Lippincott Williams & Wilkins. Copyright 2001, American Heart Association. B, Relation between coronary driving pressure (*x* axis) and normalized percent change in coronary blood flow (CBF, left *y* axis and filled circles) and MBV fraction (right *y* axis and open circles) over a wide range of coronary driving pressures in dogs. The shaded area denotes the autoregulatory range. See text for details. Reprinted from Le et al,[120] with permission. Copyright 2004, BMJ Publishing Group Ltd.

have been shown to have higher MBF velocity and MBV at rest, which separates them from benign tumors.[113] With the use of MCE, it has been demonstrated that the reason for the reversible defect in patients with left bundle-branch block on stress nuclear imaging is the partial volume effect caused by the poor spatial resolution of SPECT.[114] An experimental study using MCE has shown that the cyclic variation in integrated backscatter seen during the cardiac cycle is caused by cardiac contraction–induced cyclic changes in MBV and not due to cyclic alterations in myofibrillar elastic element orientation and ultrasonic anisotropy, as has been suggested previously.[115] MCE has also been used successfully to assess myocardial perfusion in both rats[116] and mice.[117]

MCE has opened up an entire new frontier of research in the control of microcirculatory flow. For instance, whole blood viscosity plays a premier role in capillary resistance, and it was shown recently that hyperlipidemia increases whole blood viscosity and decreases coronary flow reserve.[118] In this study, when serum triglyceride levels were increased during maximal hyperemia, MBF velocity decreased and myocardial vascular resistance increased (Figure 12A).

Whole blood viscosity is, in large part, determined by erythrocyte charge and deformability that ultimately affects erythrocyte mobility in capillaries. In an animal model of myocardial ischemia, it was shown that augmented MBF in the ischemic microcirculation during nitroglycerin administration occurs in tandem with increased erythrocyte *S*-nitrosothiol content that increases both erythrocyte mobility and oxygen unloading in ischemic but not nonischemic tissue.[119] Thus, when tissue is normoxic, hemoglobin binds to nitric oxide. In contradistinction, when tissue is hypoxic, hemoglobin releases nitric oxide. Thus, erythrocyte-mediated microvascular mechanisms rather than only reduction in preload and large coronary artery dilatation may contribute to the powerful anti-ischemic effects of nitroglycerin, especially during low-flow states.

Finally, it has been shown that the myocardial capillary hydrostatic pressure is tightly regulated by the body even when autoregulation is exhausted. When the coronary perfusion pressure was kept within the autoregulatory range, as expected, MBV remained unchanged (coronary blood volume increased but not MBV, which primarily reflects capillary blood volume).[120] However, when perfusion pressure was decreased, capillaries derecruited to maintain a constant hydrostatic pressure (Figure 12B). More interestingly, when aortic pressure was increased with phenylephrine, capillaries again derecruited to maintain a constant capillary hydrostatic pressure.

Remaining Challenges for MCE

Despite 25 years of research and development, MCE is not yet used routinely as a clinical tool, for which there are several reasons. First, no ultrasound contrast agent has yet been approved for myocardial opacification in the United States. The second and most important reason is that currently there is no reimbursement for MCE. In comparison, SPECT is compensated handsomely. It is also true that the learning curve for MCE is steep, and >1 person (a sonographer and an assistant/physician) is required to perform a good-quality study. Furthermore, it involves placing an intravenous line, which in many states requires the services of a registered nurse who may not be readily available. However, a fair compensation for performing and interpreting the study is likely to result in its rapid adoption.

The future of molecular imaging with MCE as a clinical entity appears uncertain at the moment. Until now, not a single human study has been performed with any of the strategies depicted in Table 2. A major reason is the reluctance to use antibodies that may inhibit activated molecules outside the myocardium and produce untoward effects. Second, even if we use other ligands instead of antibodies, a method to conjugate them to microbubbles that is safe in humans has not yet been identified. Currently, biotin-streptavidin is used for conjugating ligands to bubbles or liposomes. Streptavidin can also bind to biotin in the body (needed for fatty acid synthesis and gluconeogenesis) and prevent its function, leading to potentially deleterious effects. Conjugation of ligands to microbubbles through amine or sulfhydryl covalent bonds may be safe in humans. Although these methods may be developed soon, it will take years to

approve any one of these site-targeting agents. What is not known is whether a generic "labeling bubble" to which any small molecule can be attached will be approved or whether approval of each specific bubble-molecule combination will be required. The former would be most advantageous and would follow the model of PET, in which isotopes can be produced "in-house" and labeled with compounds, whereas the latter may be too daunting to pursue.

Summary

It is remarkable that there is already a vast literature, including large studies, showing the diagnostic and prognostic value of MCE even before a single ultrasound contrast agent has been approved in the United States for this purpose. The response of the US Food and Drug Administration to phase III study results of Cardiosphere and Imagify and subsequent reimbursement for MCE will determine its clinical adoption and success. Whether MCE develops into a universally applied clinical tool or not, it has been a valuable experimental tool for the discovery of new physiological and pathophysiological insights into the microcirculation and local control of MBF. Some of these have been described previously and some in this review. For a relatively inexpensive tool, MCE can provide rather sophisticated information in individual patients in various clinical scenarios. Its greater clinical adoption can only enhance patient care.

Acknowledgments

The work cited herein reflects the hard work by many colleagues here at Oregon Health and Science University and elsewhere as well as many postdoctoral fellows who have worked in laboratories of several investigators over many years. The true acknowledgement of their work is in the references cited here and in previous reviews (page and reference limits precluded many important articles from being cited here).

Sources of Funding

This work was supported by grants (R01-EB-002069, R01-HL-65704, and R01-HL-66034) from the National Institutes of Health, Bethesda, Md.

Disclosures

None.

References

1. Kaul S. Myocardial contrast echocardiography: 15 years of research and development. *Circulation*. 1997;96:3745–3760.
2. Kaul S, Ito H. The microvasculature in acute myocardial ischemia: evolving concepts in pathophysiology, diagnosis, and treatment, part I. *Circulation*. 2003;109:146–149.
3. Kaul S, Ito H. The microvasculature in acute myocardial ischemia: evolving concepts in pathophysiology, diagnosis, and treatment, part II. *Circulation*. 2003;109:310–315.
4. Armstrong WF, Mueller TM, Kinney EL, Tickner EG, Dillon JC, Feigenbaum H. Assessment of myocardial perfusion abnormalities with contrast-enhanced two-dimensional echocardiography. *Circulation*. 1982;66:166–173.
5. Kemper AJ, O'Boyle JE, Cohen CA, Taylor A, Parisi AF. Hydrogen peroxide contrast echocardiography: quantification in vivo of myocardial risk area during coronary occlusion and the necrotic area remaining after myocardial reperfusion. *Circulation*. 1984;70:309–317.
6. Kaul S, Pandian NG, Okada RD, Pohost GM, Weyman AE. Contrast echocardiography in acute myocardial ischemia, I: in-vivo determination of total left ventricular "area at risk." *J Am Coll Cardiol*. 1984;4:1272–1282.
7. Kaul S, Pandian NG, Gillam LD, Newell JB, Okada RD, Weyman AE. Contrast echocardiography in acute myocardial ischemia, III: an in-vivo comparison of the extent of abnormal wall motion with the area at risk for necrosis. *J Am Coll Cardiol*. 1986;7:383–392.
8. Kaul S, Glasheen W, Ruddy TD, Pandian NG, Weyman AE, Okada RD. The importance of defining left ventricular 'area at risk' in-vivo during acute myocardial infarction: an experimental evaluation utilizing myocardial contrast 2D-echocardiography. *Circulation*. 1987;75:1249–1260.
9. Kaul S, Pandian NG, Guerrero JL, Gillam LD, Okada RD, Weyman AE. Effects of selectively altering the collateral driving pressure on regional perfusion and function in the occluded coronary bed in the dog. *Circ Res*. 1987;61:77–85.
10. Feinstein SB, Ten Cate F, Zwehl W, Ong K, Maurer G, Tei C, Shah PM, Meerbaum S, Corday E. Two-dimensional contrast echocardiography, I: in vitro development and quantitative analysis of echo contrast agents. *J Am Coll Cardiol*. 1984;3:14–20.
11. Keller MW, Glasheen W, Teja K, Gear A, Kaul S. Myocardial contrast echocardiography without significant hemodynamic effects or reactive hyperemia: a major advantage in the imaging of myocardial perfusion. *J Am Coll Cardiol*. 1988;12:1039–1047.
12. Moore CA, Smucker ML, Kaul S. Myocardial contrast echocardiography in humans, I: safety: a comparison with routine coronary arteriography. *J Am Coll Cardiol*. 1986;8:1066–1072.
13. Keller MW, Glasheen WP, Smucker ML, Burwell LR, Watson DD, Kaul S. Myocardial contrast echocardiography in humans, II: assessment of coronary blood flow reserve. *J Am Coll Cardiol*. 1988;12:924–935.
14. Keller MW, Glasheen WP, Kaul S. Albunex: a safe and effective commercially produced agent for myocardial contrast echocardiography. *J Am Soc Echocardiogr*. 1989;2:48–52.
15. Lindner JR, Dent JM, Moos S, Jayaweera AR, Kaul S. Enhancement of left ventricular cavity opacification by harmonic imaging after venous injection of Albunex. *Am J Cardiol*. 1997;79:1657–1662.
16. Klibanov AL, Hughes MS, Wojdyta J, Wible J, Brandenburg G. Destruction of contrast agent microbubbles in the ultrasound field: the fate of microbubble shell and the importance of bubble gas content. *Acad Radiol*. 2002;9:S41–S45.
17. Postema H, vanWamel A, ten Cate FJ, de Jong N. High-speed photography during ultrasound illustrates potential therapeutic applications of microbubbles. *Med Phys*. 2005;32:3707–3711.
18. Skyba DM, Camarano G, Goodman NC, Price RJ, Skalak TC, Kaul S. Hemodynamic characteristics, myocardial kinetics, and microvascular rheology of FS-069, a second-generation echocardiographic contrast agent capable of producing myocardial opacification from a venous injection. *J Am Coll Cardiol*. 1996;28:1292–1300.
19. Lindner JR, Firschke C, Wei K, Goodman NC, Skyba DM, Kaul S. Myocardial perfusion characteristics and hemodynamic profile of MRX-115, a venous echocardiographic contrast agent, during acute myocardial infarction. *J Am Soc Echocardiogr*. 1998;11:36–46.
20. Keller MW, Segal SS, Kaul S, Duling B. The behavior of sonicated albumin microbubbles within the microcirculation: a basis for their use during myocardial contrast echocardiography. *Circ Res*. 1989;65:458–467.
21. Lindner JR, Song J, Jayaweera AR, Sklenar J, Kaul S. Microvascular rheology of Definity microbubbles after intra-arterial and intravenous administration. *J Am Soc Echocardiogr*. 2002;15:396–403.
22. Jayaweera AR, Edwards N, Glasheen WP, Villanueva FS, Abbott RD, Kaul S. In-vivo myocardial kinetics of air-filled albumin microbubbles during myocardial contrast echocardiography: comparison with radiolabeled red blood cells. *Circ Res*. 1994;74:1157–1165.
23. Wei K, Skyba DM, Firschke C, Lindner JR, Jayaweera AR, Kaul S. Interaction between microbubbles and ultrasound: in vitro and in vivo observations. *J Am Coll Cardiol*. 1997;29:1081–1088.
24. Uhlendorf V, Hoffman C. Nonlinear acoustical response of coated microbubbles in diagnostic ultrasound. *IEEE Proc*. 1994;3:1559–1562.
25. Shi W, Forsberg F. Ultrasonic characterization of the nonlinear properties of contrast microbubbles. *Ultrasound Med Biol*. 2000;26:93–104.
26. Kaul S. Instrumentation for contrast echocardiography: technology and techniques. *Am J Cardiol*. 2002;90(suppl) 8J–14J.
27. Lindner JR, Villanueva FS, Dent JM, Wei K, Sklenar J, Kaul S. Assessment of resting perfusion with myocardial contrast echocardiography: theoretical and practical considerations. *Am Heart J*. 2000;139:231–240.

28. Wei K, Jayaweera AR Firoozan S, Linka A, Skyba DM, Kaul S. Quantification of myocardial blood flow with ultrasound-induced destruction of microbubbles administered as a constant venous infusion. *Circulation*. 1998;97:473–483.
29. Le DE, Bin JP, Coggins M, Linder J, Wei K, Kaul S. Relation between myocardial oxygen consumption and myocardial blood volume: a study using myocardial contrast echocardiography. *J Am Soc Echocardiogr*. 2002;15:857–863.
30. Toyota E, Fujimoto K, Ogasawara Y, Kajita T, Shigeto F, Matsumoto T, Goto M, Kajiya F. Dynamic changes in three-dimensional architecture and vascular volume of transmural coronary microvasculature between diastolic- and systolic-arrested rat hearts. *Circulation*. 2002;105:621–626.
31. Vogel R, Indermühle A, Reinhardt J, Meier P, Siegrist PT, Namdar M, Kaufmann PA, Seiler C. The quantification of absolute myocardial perfusion in humans by contrast echocardiography: algorithm and validation. *J Am Coll Cardiol*. 2005;45:754–762.
32. Jayaweera AR, Wei K, Coggins M, Bin JP, Goodman C, Kaul S. Role of capillaries in determining coronary blood flow reserve: new insights using myocardial contrast echocardiography. *Am J Physiol*. 1999;277:H2363–H2372.
33. Wei K, Le E, Min JP, Coggins M, Goodman NC, Kaul S. Mechanism of reversible ^{99m}Tc-sestamibi perfusion defects during pharmacologically-induced coronary vasodilatation. *Am J Physiol*. 2001,280:H1896–H1904.
34. Bin JP, Le DE, Jayaweera AR, Coggins MP, Wei K, Kaul S. Direct effects of dobutamine on the coronary microcirculation: comparison with adenosine using myocardial contrast echocardiography. *J Am Soc Echocardiogr*. 2003;16:871–879.
35. Bin JP, Pelberg RA, Coggins MP, Wei K, Kaul S. Mechanism of inducible regional dysfunction during dipyridamole stress. *Circulation*. 2002;106:112–117.
36. Miszalski-Jamka T, Kuntz-Hehner S, Schmidt H, Hammerstingl C, Tiemann K, Ghanem A, Troatz C, Lüderitz B, Omran H. Real time myocardial contrast echocardiography during supine bicycle stress and continuous infusion of contrast agent: cutoff values for myocardial contrast replenishment discriminating abnormal myocardial perfusion. *Echocardiography*. 2007;24:638–648.
37. Bin JP, Pelberg RA, Wei K, Le DE, Goodman NC, Kaul S. Dobutamine versus dipyridamole for inducing reversible perfusion defects in chronic multivessel coronary artery stenosis. *J Am Coll Cardiol*. 2002;40:167–174.
38. Ito H, Tomooka T, Sakai N, Yu H, Higashino Y, Fujii K, Masuyama T, Kitabatake A, Minamino T. Lack of myocardial perfusion immediately after successful thrombolysis: a predictor of poor recovery of left ventricular function in anterior myocardial infarction. *Circulation*. 1992;85:1699–1705.
39. Ito H, Maruyama A, Iwakura K, Takiuchi S, Masuyama T, Hori M, Higashino Y, Fujii K, Minamino T. Clinical implications of the "no reflow" phenomenon: a predictor of complications and left ventricular remodeling in reperfused anterior wall myocardial infarction. *Circulation*. 1996;93:223–228.
40. Ragosta M, Camarano GP, Kaul S, Powers E, Sarembock IJ, Gimple LW. Microvascular integrity indicates myocellular viability in patients with recent myocardial infarction: new insights using myocardial contrast echocardiography. *Circulation*. 1994;89:2562–2569.
41. Sakuma T, Hayashi Y, Sumii K, Imazu M, Yamakido M. Prediction of short- and intermediate-term prognoses of patients with acute myocardial infarction using myocardial contrast echocardiography one day after recanalization. *J Am Coll Cardiol*. 1998;32:890–897.
42. Villanueva FS, Glasheen WP, Sklenar J, Kaul S. Characterization of spatial patterns of flow within the reperfused myocardium using myocardial contrast echocardiography: implications in determining the extent of myocardial salvage. *Circulation*. 1993;88:2596–2606.
43. Villanueva FS, Camarano G, Ismail S, Goodman NC, Sklenar J, Kaul S. Coronary reserve abnormalities during post-infarct reperfusion: implications for the timing of myocardial contrast echocardiography to assess myocardial viability. *Circulation*. 1996;94:748–754.
44. Sabia PJ, Powers ER, Ragosta M, Sarembock IJ, Burwell LR, Kaul S. An association between collateral blood flow and myocardial viability in patients with recent myocardial infarction. *N Engl J Med*. 1992;372:1825–1831.
45. Sabia PJ, Powers ER, Jayaweera AR, Ragosta M, Kaul S. Functional significance of collateral blood flow in patients with recent acute myocardial infarction: a study using myocardial contrast echocardiography. *Circulation*. 1992;85:2080–2089.
46. Coggins MP, Le DE, Wei K, Goodman NC, Lindner JR, Kaul S. Noninvasive prediction of ultimate infarct size at the time of acute coronary occlusion based on the extent and magnitude of collateral-derived myocardial blood flow. *Circulation*. 2001;104:2471–2477.
47. Janardhanan R, Swinburn JM, Greaves K, Senior R. Usefulness of myocardial contrast echocardiography using low-power continuous imaging early after acute myocardial infarction to predict late functional left ventricular recovery. *Am J Cardiol*. 2003;92:493–497.
48. Dwivedi G, Janardhanan R, Hayat SA, Swinburn JA, Senior R. Prognostic value of myocardial viability detected by myocardial contrast echocardiography early after acute myocardial infarction. *J Am Coll Cardiol*. 2007;50:327–334.
49. Hayat SA, Janardhanan R, Moon JC, Pennell DJ, Senior R. Comparison between myocardial contrast echocardiography and single-photon emission computed tomography for predicting transmurality of acute myocardial infarction. *Am J Cardiol*. 2006;97:1718–1721.
50. Rovai D, Zanchi M, Lombardi M, Magagnini E, Chella P, Pieroni A, Picano E, Ferdeghini M, Morris H, Distante A, L'Abbate A. Residual myocardial perfusion in reversibly damaged myocardium by dipyridamole contrast echocardiography. *Eur Heart J*. 2006;17:296–301.
51. Galiuto L, Gabrielli FA, Lombardo A, La Torre G, Scara A, Rebuzzi AG, Crea F. Reversible microvascular dysfunction coupled with persistent myocardial dysfunction: implications for post-infarct left ventricular remodelling. *Heart*. 2007;93:565–571.
52. Ujino K, Hillis GS, Mulvagh SL, Hagen ME, Oh JK. Usefulness of real-time intravenous myocardial contrast echocardiography in predicting left ventricular dilation after successfully reperfused acute myocardial infarction. *Am J Cardiol*. 2005;96:17–21.
53. Scherrer-Crosbie M, Liel-Cohen N, Otsuji Y, Guerrero JL, Sullivan S, Levine RA, Picard MH. Myocardial perfusion and wall motion in infarction border zone: assessment by myocardial contrast echocardiography. *J Am Soc Echocardiogr*. 2000;13:353–357.
54. Leong-Poi H, Coggins M, Sklenar J, Jayaweera AR, Wang X, Kaul S. Role of collateral blood flow in the apparent disparity between the extent of abnormal wall thickening and perfusion defect size during acute myocardial infarction and demand ischemia. *J Am Coll Cardiol*. 2005;45:565–572.
55. Kaul S, Senior R, Firschke C, Wang X, Lindner JR, Villanueva FS, Kontos MC, Taylor A, Nixon JV, Watson DD, Harrell FE. Incremental value of cardiac imaging in patients presenting to the emergency department with chest pain and without ST-segment elevation: a multicenter study. *Am Heart J*. 2004;148:129–136.
56. Korosoglou G, Labadze N, Hansen A, Selter C, Giannitsis E, Katus H, Kuecherer H. Usefulness of real-time myocardial perfusion imaging in the evaluation of patients with first time chest pain. *Am J Cardiol*. 2004;94:1225–1231.
57. Rinkevich D, Kaul S, Wang X-Q, Tong KL, Belcik T, Kalvaitis S, Lepper W, Foster WA, Wei K. Incremental value of regional perfusion over regional function in patients presenting to the emergency department with suspected cardiac chest pain and non-diagnostic electrocardiographic changes. *Eur Heart J*. 2005;26:1606–1611.
58. Tong KL, Kaul S, Wang X, Rinkevich A, Kalvaitis S, Belcik T, Lepper W, Foster WA, Wei K. Myocardial contrast echocardiography provides superior and rapid prognostic information compared to routine assessment in patients presenting with chest pain to the emergency department. *J Am Coll Cardiol*. 2005;46:920–927.
59. Senior R, Ashrafian H. Detecting acute coronary syndrome in the emergency department: the answer is in seeing the heart: why look further? *Eur Heart J*. 2005;26:1606–1611.
60. Vannan MA, Narula J. Ischemic versus nonischemic chest pain in the emergency room. *J Am Coll Cardiol*. 2005;46:928–929.
61. Ramakrishna G, Ravi BS, Chandrasekaran K. Apical ballooning syndrome in a postoperative patient with normal microvascular perfusion by myocardial contrast echocardiography. *Echocardiography*. 2005;22:606–610.
62. Ismail S, Jayaweera AR, Goodman NC, Camarano GP, Skyba DM, Kaul S. Detection of coronary artery stenoses and quantification of blood flow mismatch during coronary hyperemia with myocardial contrast echocardiography. *Circulation*. 1995;91:821–830.
63. Firschke C, Lindner JR, Wei K, Skyba D, Goodman NC, Kaul S. Myocardial perfusion imaging in the setting of coronary artery stenosis and acute myocardial infarction using venous injection of FS-069, a

second generation echocardiographic contrast agent. *Circulation*. 1997; 96:959–967.
64. Wei K, Jayaweera AR, Firoozan S, Linka A, Skyba DM, Kaul S. Basis for stenosis detection using venous administration of microbubbles during myocardial contrast echocardiography: bolus or continuous infusion? *J Am Coll Cardiol*. 1998;32:252–260.
65. Kaul S, Senior R, Dittrich H, Raval U, Khattar R, Lahiri A. Detection of coronary artery disease using myocardial contrast echocardiography: comparison with ^{99m}Tc-sestamibi single photon emission computed tomography. *Circulation*. 1997;96:785–792.
66. Porter TR, Li S, Jiang L, Grayburn P, Deligonul U. Real-time visualization of myocardial perfusion and wall thickening in human beings with intravenous ultrasonographic contrast and accelerated intermittent harmonic imaging. *J Am Soc Echocardiogr*. 1999;12:266–271.
67. Wei K, Ragosta M, Thorpe J, Moos S, Kaul S. Noninvasive measurement of coronary blood flow reserve myocardial contrast echocardiography. *Circulation*. 2001;103:2560–2565.
68. Senior R, Lepper W, Pasquet A, Chung G, Hoffman R, Vanoverschelde JL, Cerquera M, Kaul S. Myocardial perfusion assessment in patients with medium probability of coronary artery disease and no prior myocardial infarction: comparison of myocardial contrast echocardiography with ^{99m}Tc-SPECT. *Am Heart J*. 2004;147:1100–1105.
69. Jeetley P, Hickman M, Kamp O, Lang RM, Thomas JD, Vannan MA, Vanoverschelde JL, van der Wouw PA, Senior R. Myocardial contrast echocardiography for the detection of coronary artery stenosis: a prospective multicenter study in comparison with single-photon emission computed tomography. *J Am Coll Cardiol*. 2006;47:141–145.
70. Dijkmans PA, Senior R, Becher H, Porter TR, Wei K, Visser CA, MD, Kamp O. Myocardial contrast echocardiography evolving as a clinically feasible technique for accurate, rapid, and safe assessment of myocardial perfusion: the evidence so far. *J Am Coll Cardiol*. 2006;48:2168–2177.
71. Senior R, Zabalgoita M, Monaghan M, Main M, Zamarano JL, Tiemann K, Agati L, Weissman NJ, Klein AL, Marwick TH, Ahmad M, DeMaria AN, Becher H, Kaul S, Udelson JE, Wackers FJ, Walvovitch RC, Picard MH. Accurate detection of coronary artery disease by echocardiography using perflubutane polymer microspheres, a novel contrast agent: comparison with nuclear perfusion imaging in two phase three multicenter clinical trials. *Circulation*. 2007;116:II-546. Abstract.
72. Bin JP, Pelberg RA, Coggins MP, Wei K, Kaul S. Mechanism of inducible regional dysfunction during dipyridamole stress. *Circulation*. 2002;106:112–117.
73. Firschke C, Andrássy P, Linka AZ, Busch R, Martinoff S. Adenosine myocardial contrast echo in intermediate severity coronary stenoses: a prospective two-center study. *Int J Cardiovasc Imaging*. 2007;23: 311–321.
74. Hauser AM, Vellappillil G, Ramos RG, Gordon S, Timmis GC. Sequence of mechanical, electrocardiographic and clinical effects of repeated coronary artery occlusion in human beings: echocardiographic observations during coronary angioplasty. *J Am Coll Cardiol*. 1985;5: 193–197.
75. Leong-Poi H, Rim S-J, Le ED, Fisher NG, Wei K, Kaul S. Perfusion versus function: the ischemic cascade in demand ischemia: implications of single- versus multivessel stenosis. *Circulation*. 2002;105:987–992.
76. Elhendy A, O'Leary EL, Xie F, McGrain AC, Anderson JR, Porter TR. Comparative accuracy of real-time myocardial contrast perfusion imaging and wall motion analysis during dobutamine stress echocardiography for the diagnosis of coronary artery disease. *J Am Coll Cardiol*. 2004;44:2185–2191.
77. Elhendy A, Tsutsui JM, O'Leary EL, Xie F, McGrain AC, Porter TR. Noninvasive diagnosis of coronary artery disease in patients with diabetes by dobutamine stress real-time myocardial contrast perfusion imaging. *Diabetes Care*. 2005;28:1662–1667.
78. Tsutsui JM, Elhendy A, Anderson JR, Xie F, McGrain AC, Porter TR. Prognostic value of dobutamine stress myocardial contrast perfusion echocardiography. *Circulation*. 2005;112:1444–1450.
79. Tsutsui JM, Xie F, Cloutier D, Kalvaitis S, Elhendy A, Porter TR. Real-time dobutamine stress myocardial perfusion echocardiography predicts outcome in the elderly. *Eur Heart J*. 2008;29:377–385.
80. Dodla S, Xie F, Cory B, Stevens RB, O'Leary E, Porter TR. Prognostic value and angiographic correlation of dobutamine stress imaging with real time perfusion echocardiography in asymptomatic diabetic patients undergoing pre-operative evaluation. *J Am Soc Echocardiogr*. 2007; 20:564. Abstract.
81. Moir S, Haluska B, Jenkins C, McNab D, Marwick TH. Comparison of specificity of quantitative myocardial contrast echocardiography for diagnosis of coronary artery disease in patients with versus without diabetes mellitus. *Am J Cardiol*. 2005;96:187–192.
82. Tsutsui JM, Mukherjee S, Elhendy A, Xie F, Lyden ER, O'Leary E, McGrain AC, Porter TR. Value of dobutamine stress myocardial contrast perfusion echocardiography in patients with advanced liver disease. *Liver Transplantation*. 2006;12:592–599.
83. Lindner JR, Skyba DM, Goodman NC, Jayaweera AR, Kaul S. Changes in myocardial blood volume with graded coronary stenosis: an experimental evaluation using myocardial contrast echocardiography. *Am J Physiol*. 1997;272:H567–H575.
84. Wei K, Le E, Bin JP, Jayaweera AR, Goodman NC, Kaul S. Noninvasive detection of coronary artery stenosis at rest without recourse to exercise or pharmacologic stress. *Circulation*. 2002;105:218–223.
85. Wei K, Tong KL, Belcik T, Rafter P, Ragosta M, Kaul S. Detection of non-critical coronary stenosis at rest with myocardial contrast echocardiography. *Circulation*. 2005;112:1154–1160.
86. Grayburn PA. Stress echo without the stress: detection of coronary stenosis at rest by myocardial contrast echocardiography. *Circulation*. 2005;112:1085–1087.
87. Pascotto M, Wei K, Micari A, Bragadeesh T, Goodman NC, Kaul S. Phasic changes in myocardial blood volume are influenced by collateral blood flow: implications for the quantification of coronary stenosis at rest. *Heart*. 2007;93:438–443.
88. Shimoni S, Fangogiannis NG, Aggeli CJ, Shan K, Verani MS, Quinones MA, Espada R, Letsou GV, Lawrie GM, Winters WL, Reardon MJ, Zoghbi WA. Identification of hibernating myocardium with quantitative intravenous myocardial contrast echocardiography comparison with dobutamine echocardiography and thallium-201 scintigraphy. *Circulation*. 2003;107:538–544.
89. Shimoni S, Frangogiannis NG, Aggeli CJ, MD, Shan K, Quinones MA, Espada R, Letsou GV, Lawrie GM, Winters WL, Reardon MJ, Zoghbi WA. Microvascular structural correlates of myocardial contrast echocardiography in patients with coronary artery disease and left ventricular dysfunction implications for the assessment of myocardial hibernation. *Circulation*. 2002;106:950–956.
90. Senior R, Janardhanan R, Jeetley P, Burden L. Myocardial contrast echocardiography for distinguishing ischemic from nonischemic first-onset acute heart failure insights into the mechanism of acute heart failure. *Circulation*. 2005;112:1587–1593.
91. Keller MW, Spotnitz WD, Matthew TL, Glasheen WP, Watson DD, Kaul S. Intraoperative assessment of regional myocardial perfusion using quantitative myocardial contrast echocardiography: an experimental evaluation. *J Am Coll Cardiol*. 1990;16:1267–1279.
92. Villanueva FS, Spotnitz WD, Jayaweera AR, Gimple LW, Dent J, Kaul S. On-line intraoperative quantitation of regional myocardial perfusion during coronary artery bypass graft operations with myocardial contrast two-dimensional echocardiography. *J Thorac Cardiovasc Surg*. 1992; 104:1524–1531.
93. Bayfield M, Lindner JR, Kaul S, Ismail S, Goodman NC, Spotnitz WD. Deoxygenated blood minimizes adherence of sonicated albumin microbubbles during cardioplegic arrest and after blood reperfusion: experimental and clinical observations with myocardial contrast echocardiography. *J Thorac Cardiovasc Surg*. 1997;113:1100–1108.
94. Lindner JR, Coggins MP, Kaul S, Klibanov AL, Brandenburger GH, Ley K. Microbubble persistence in the microcirculation during ischemia-reperfusion and inflammation is caused by integrin- and complement-mediated adherence to activated leukocytes. *Circulation*. 2000;101:668–675.
95. Leong-Poi H, Christiansen J, Klibanov AL, Kaul S, Lindner JR. Noninvasive assessment of angiogenesis by molecular imaging with ultrasound and microbubbles targeted to α_v integrins. *Circulation*. 2003; 107:455–460.
96. Ellegala DB, Leong-Poi H, Carpenter JE, Klibanov AL, Kaul S, Shaffrey ME, Sklenar J, Lindner JR. Imaging tumor angiogenesis with contrast ultrasound and microbubbles targeted to $\alpha_{v\beta3}$. *Circulation*. 2003;108:336–341.
97. Weller GER, Wong MKK, Modzelewski RA, Lu E, Klibanov AL, Wagner WR, Villanueva FS. Ultrasonic imaging of tumor angiogenesis using contrast microbubbles targeted via the tumor-binding peptide arginine-arginine-leucine. *Cancer Res*. 2005;65:533–539.
98. Villanueva FS, Jankowski RJ, Klibanov S, Pina ML, Alber SM, Watkins SC, Brandenburger GH, Wagner WR. Microbubbles targeted to intercellular adhesion molecule-1 bind to activated coronary artery endothelial cells. *Circulation*. 1998;98:1–5.

99. Weller GER, Lu E, Csikari MM, Klibanov AL, Fischer D, Wagner WR, Villanueva FS. Ultrasound imaging of acute cardiac transplant rejection with microbubbles targeted to intercellular adhesion molecule-1. *Circulation*. 2003;108:218–224.
100. Lindner JR, Dayton PA, Coogins MP, Ley K, Song J, Ferrara K, Kaul S. Noninvasive imaging of inflammation by ultrasound detection of phagocytosed microbubbles. *Circulation*. 2000;102:531–538.
101. Lindner JR, Song J, Xu F, Klibanov AL, Singbartl K, Ley K, Kaul S. Noninvasive ultrasound imaging of inflammation using microbubbles targeted to activated leukocytes. *Circulation*. 2000;102:2745–2750.
102. Christiansen JP, Leong-Poi H, Klibanov AL, Kaul S, Lindner JR. Noninvasive imaging of myocardial reperfusion injury using leukocyte-targeted contrast echocardiography. *Circulation*. 2002;105:1764–1767.
103. Schumann P, Christiansen JP, Quigley RM, McCreery TP, Sweitzer RH, Unger EC, Lindner JR, Matsunaga TO. Targeted-microbubble binding selectively to GPIIb IIIa receptors of platelet thrombi. *Invest Radiol*. 2002;37:587–593.
104. Sakuma T, Sklenar J, Leong-Poi H, Goodman NC, Glover DK, Kaul S. Molecular imaging identifies regions with microthromboemboli during primary angioplasty in acute coronary thrombosis. *J Nucl Med*. 2004; 45:1194–1200.
105. Villanueva FS, Lu E, MD, Bowry S, Kilic S, Tom E, Wang J, Gretton J, Pacella JJ, Wagner WR. Myocardial ischemic memory imaging with molecular echocardiography. *Circulation*. 2007;115:345–352.
106. Kaufmann B, Lewis C, Xie A, Mirza-Mohd A, Lindner JR. Detection of recent myocardial ischaemia by molecular imaging of P-selectin with targeted contrast echocardiography. *Eur Heart J*. 2007;28:2011–2017.
107. Kaufmann BA, Sanders JM, Davis C, Xie A, Aldred P, Sarembock IJ, Lindner JR. Molecular imaging of inflammation in atherosclerosis with targeted ultrasound detection of vascular cell adhesion molecule-1. *Circulation*. 2007;116:276–284.
108. Anderson DR, Tsutsui JM, Xie F, Radio SJ, Porter TR. The role of complement in the adherence of microbubbles to dysfunctional arterial endothelium and atherosclerotic plaque. *Cardiovasc Res*. 2007;73: 597–606.
109. Sakuma T, Sari I, Goodman NC, Lindner JR, Klibanov A, Kaul S. Simultaneous $\alpha_{v\beta3}$ and IIb/IIIa inhibition causes a marked reduction in infarct size following reperfusion in a canine model of acute coronary thrombosis: utility of in-vivo molecular imaging with myocardial contrast echocardiography. *Cardiovasc Res*. 2005;66:552–561.
110. Nagueh SF, Lakkis NM, Zuo-Xiang H, Middleton KJ, Killip A, Zoghbi WA, Quinones MA, Roberts E, Verani MS, Kleiman NS. Role of myocardial contrast echocardiography during nonsurgical septal reduction therapy for hypertrophic obstructive cardiomyopathy. *J Am Coll Cardiol*. 1998;32:225–229.
111. Masugata H, Fujita N, Kondo I, Peters B, Ohmori K, Mizushige K, Kohno M, DeMaria AN. Assessment of right ventricular perfusion after right coronary artery occlusion by myocardial contrast echocardiography. *J Am Coll Cardiol*. 2003;41:1823–1830.
112. Wolf D, Reinhard A, Krause U, Seckinger A, Katus HA, Kuecherer H, Hansen A. Stem cell therapy improves myocardial perfusion and cardiac synchronicity: new application for echocardiography. *J Am Soc Echocardiogr*. 2007;20:512–520.
113. Kirkpatrick JN, Wong T, Bednarz JE, Spencer KT, Sugeng L, Ward RP, DeCara JM, Weinert L, Krausz T, Lang RM. Differential diagnosis of cardiac masses using contrast echocardiographic perfusion imaging. *J Am Coll Cardiol*. 2004;43:1412–1419.
114. Hayat SA, Dwivedi G, Jacobson A, Kinsey C, Senior R. Effects of left bundle branch block on cardiac structure, function, perfusion and perfusion reserve: implications for myocardial contrast echocardiography versus radionuclide perfusion imaging for the detection of coronary artery disease. *Circulation*. 2008;117:1832–1841.
115. Micari A, Pascotto M, Jayaweera AR, Sklenar J, Goodman NC, Kaul S. Cyclic variation in ultrasonic myocardial integrated backscatter is due to phasic changes in myocardial microvascular dimensions. *J Ultrasound Med*. 2006;25:1009–1019.
116. Thibault H, Lafitte S, Timperley J, Tariosse L, Becher H, Roudaut R. Dos Santos P. Quantitative analysis of myocardial perfusion in rats by contrast echocardiography. *J Am Soc Echocardiogr*. 2005;18: 1321–1328.
117. Kaufmann BA, Lankford M, Behm CZ, French BA, Klibanov AL, Xu Y, Lindner JR. High-resolution myocardial perfusion imaging in mice with high-frequency echocardiographic detection of a depot contrast agent. *J Am Soc Echocardiogr*. 2007;20:136–43.
118. Rim S-J, Leong-Poi H, Lindner JR, Wei K, Fisher NG, Kaul S. The decrease in coronary blood flow reserve during hyperlipidemia is secondary to an increase in blood viscosity. *Circulation*. 2001;104: 2704–2709.
119. Bin JP, Doctor A, Lindner JR, Leong-Poi H, Fisher NG, Le ED, Hendersen EH, Christiansen J, Kaul S. Effects of nitroglycerin on erythrocyte rheology and oxygen unloading: novel role of S-nitrosohemoglobin in relieving myocardial ischemia. *Circulation*. 2006;113:2502–2508.
120. Le DE, Jayaweera AR, Wei K, Coggins MP, Lindner JR, Kaul S. Changes in myocardial blood volume over a wide range of coronary driving pressures: role of capillaries beyond the autoregulatory range. *Heart*. 2004;90:1199–1205.

KEY WORDS: contrast media ■ coronary disease ■ echocardiography ■ imaging